Title:

The response of desert biocrust bacterial communities to hydration-desiccation cycles

Authors:

Capucine Baubin[§], Noya Ran, Hagar Siebner, Osnat Gillor[§]

Affiliation:

Zuckerberg Institute for Water Research, Blaustein Institutes for Desert Research, Ben-Gurion University of the Negev, 8499000, Israel

Corresponding authors:

[§]Capucine Baubin, Zuckerberg Institute for Water Research, Blaustein Institutes for Desert Research, Ben-Gurion University of the Negev, 8499000, Israel. Tel: 972-8-6596363; e-mail: baubin@bgu.ac.il

[§]Osnat Gillor, Zuckerberg Institute for Water Research, Blaustein Institutes for Desert Research, Ben-Gurion University of the Negev, 8499000, Israel. Tel: 972-8-6596986; e-mail: gilloro@bgu.ac.il

ABSTRACT

Rain events in arid environments are highly unpredictable, interspersing extended periods of drought. Therefore, following changes in desert soil bacterial communities during hydration-desiccation cycles in the field, was seldom attempted. Here, we assessed rain-mediated dynamics of active community in the Negev Desert biological soil crust (biocrust), and evaluated the changes in bacterial composition, potential function, and photosynthetic activity. We predicted that increased biocrust moisture would resuscitate the phototrophs, while desiccation would inhibit their activity. Our results show that hydration increased chlorophyll content, resuscitated the biocrust *Cyanobacteria*, and induced potential phototrophic functions. However, decrease in the soil water content did not immediately decrease the phototrophs activity, though chlorophyll levels decreased. Moreover, while the *Cyanobacteria* relative abundance significantly increased, *Actinobacteria*, the former dominant taxa, significantly decreased in abundance. We propose that, following a rain event biocrust moisture significantly decreased, almost to drought levels, yet the response of the active bacterial community lagged, in contrast to topsoil. Possible explanations to the described rain-mediated bacteria dynamics are discussed.

Key words: hydration; biocrust; bacteria; *Cyanobacteria*; *Actinobacteria*;

1. INTRODUCTION

Arid environments are the largest terrestrial biomes on Earth and accounts for 35% of the landmass (Pointing and Belnap, 2012). Since rain in arid environments is rare and unpredictable, the main source of water is dew (Malek et al., 1999) and fog (Kidron et al., 2002). This moisture is readily absorbed to the soil surface, but would quickly evaporates due to high temperatures and low humidity (Cameron and Blank, 1966). The long droughts in drylands limit plant growth and in their stead, the soil is covered by microbial mats, called biological soil crust (biocrust). Biocrusts are a matrix of phototroph and heterotroph microorganisms that bind together with soil particles, by using extracellular polymeric substances (EPS) (Belnap and Lange, 2001; Campbell et al., 1989; Kidron et al., 2020). Biocrust phototrophs are the main primary producers in this desolate habitat and together with the heterotrophs form a rigid and stable mat that is able to resist to xerification and soil erosion (Aanderud et al., 2019; Bowker et al., 2018).

Biocrusts are the main source of carbon and nitrogen (Agarwal et al., 2014), and a strong contributor of soil respiration (Castillo-Monroy et al., 2011) in deserts. It was recently shown that, during long droughts many of the biocrust microorganisms rely not only on photosynthesis but also on oxidation of atmospheric trace gases (Leung et al., 2020; Meier et al., 2021). Yet, once the biocrust is hydrated, the phototrophs respond quickly by inducing their photosynthetic systems and related functions to take full advantage of the rare water abundance before the soil dehydrates (Murik et al., 2017). To that end, photosynthetic members of the biocrust community form a seed bank of species that are able to spring to life whenever the water content increases (Kedem et al., 2020; Lennon and Jones, 2011; Murik et al., 2017). Yet, the abrupt hydration may also cause osmotic shock that could result in massive cell lysis and the release of osmoregulatory solutes (Halverson et al., 2000; Harris,

1981). The period of water abundance is usually brief, and the soil quickly dehydrates forcing the bacteria to cease their activity (Murik et al., 2017; Oren et al., 2019). Therefore, the members of the biocrust community must respond quickly and efficiently not only to hydration but also to the subsequent desiccation.

Earlier studies focused on community structure and cyanobacterial response to hydration-desiccation cycles under controlled conditions (Angel and Conrad, 2013; Meier et al., 2020; Oren et al., 2019; Wu et al., 2013). To the best of our knowledge, these cycles were never monitored in the field during a rain event. Under natural conditions, the biocrust community dynamics of the hydration-desiccation cycle may be affected by plethora of variables, such as temperature, rain intensity, or soil local structure, which could not be applied in a laboratory setting. Thus, it is imperative to elucidate the resuscitated community and its response to the gradual dehydration after a rain event in the field.

In this study, we followed the community structure and activity before, during, and after a rain event in the arid Negev Desert (Israel). We studied the active biocrust community by using SSU ribosomes as a proxy to active bacterial community (Šťovíček et al., 2017). Although ribosomes do not quickly degrade in dormant or even dead cells (Sukenik et al., 2012; Sunyer-Figueres et al., 2018), under field conditions they present a reliable mean to distinguish between active and inactive cells (Angel et al., 2013; Šťovíček et al., 2017). We hypothesised that the biocrust community would quickly respond to hydration and to desiccation. We predicted that high soil moisture would trigger photosynthetic activity and a decreasing soil moisture will lead to an inactivation of the phototrophs within the biocrust community. We further predicted that heterotrophs response to hydration-desiccation would differ among phyla as previously reported for biocrust (Angel and Conrad, 2013) and topsoil

(Šťovíček et al., 2017) collected from the same site. The most apparent change detected in both soil horizons was the sharp decrease in the relative abundance of *Actinobacteria* that dominant the soil during droughts but decline upon hydration.

2. MATERIAL AND METHODS

2.1. Sampling

The study was conducted in the long-term ecological research station in the Negev Desert Highlands (Zin Plateau, 30°86'N, 34°80'E, Israel; Figure 1). In this arid environment, the average annual rainfall is around 90 mm and extends from October to April. Biocrust samples were collected on 20/06/17 during the dry season (T[0]; average temperature: 32.4°C) and during a rain event in the wet season from 29/01/18 through 01/02/18 at 24 hr intervals. The rain event (5.1 mm, maximum average temperature 14.6 °C) occurred 29/01/18 (T[R]) and samples were collected till the biocrust dried (T[1], T[2], T[3]; Figure 1) For each time point, five samples at least 10 m apart were collected (N = 25 samples). The biocrust samples were homogenised using a 2 mm sieve and then four subsamples were stored: (1) at -80°C for molecular analysis; (2) at -20°C for chlorophyll extraction; (3) at 60°C for 3 days and then kept at room temperature for chemical analysis; and (4) was used immediately to evaluate the water content.

2.2. Physico-chemical analyses

Water content, organic carbon and total nitrogen were measured in the soil samples. Biocrust water content was determined by the gravimetric method, the soil was weighed before and after oven drying at 105 C, then the percentage of moisture in the soil was determined (Scrimgeour, 2008). Organic carbon content was determined using the loss-on-ignition method. 30 g of the dry soil sample was weighedburnt at 380°C for 6 hours, and the fraction of organic carbon content was calculated as previously described (Hoogsteen et al., 2015; Scrimgeour, 2008). Total nitrogen was measured in 50 mg of soil using the FlashSmart CHNS/O elemental analyser (ThermoFischer, Waltham, MA, USA). The standards: BBOT

(2,5-Bis (5-tert-butyl-benzoxazol-2-yl) thiophene), Tocopherol Nicotinate and a soil reference material were used to calibrate the instrument.

2.3. Chlorophyll concentration and water content

The chlorophyll of each sample was extracted using a protocol based on Castle et al., (2010) and Ritchie, (2006). The extraction was done using methanol, with a soil:methanol ratio of 3:9, followed by a 15-minutes incubation at 65°C and a 2-hour incubation at 4°C. The samples were measured by spectrophotometry at 665 nm and the concentration of chlorophyll was calculated following Ritchie, (2006). Positive controls were spirulina with a concentration of 0.003g/g of soil and negative controls were distilled water. The concentrations are presented in mg of chlorophyll per gram of soil (mg chla/g soil).

2.4. RNA extraction and preparation for sequencing

RNA was extracted from 0.5 – 1 g of soil using phenol-chloroform, following the protocol from Angel (2012). The extracted total nucleic acid was treated with DNase to remove the DNA. The remaining RNA was cleaned using parts of the *MagListo* RNA Extraction kit (Bioneer, Daejeon, South Korea). The RNA was reverse transcribed to cDNA using Superscript IV (ThermoFischer, Waltham, MA, USA), and purified using the PCR purification kit (Bioneer, Daejeon, South Korea) in accordance with the manufacturers' instructions. The cDNA was used as a template to amplify the V3F(341) and V4R(806) regions of the 16S rRNA with CS1/CS2 extensions (Table A.1), in triplicates. Library preparations and sequencing were performed at the Research Resource Centre at the University of Illinois with pair end (2 x 300 bp) MiSeq platform (Illumina, San Diego, CA, USA). Due to low concentrations of ribosomes in the dry soil collected during the summer of 2017, we had to re-extract and re-sequence these samples. However, COVID-19 restrictions

prohibit us from using the same sequencing platform, and we were forced to use the facilities and resources available to us at the time. Therefore, RNA was extracted using the RNeasy PowerSoil Total RNA Kit (Qiagen, Hilden, Germany), following the manufacturer's protocol. Then, the V3-V4 region of the 16S rRNA was amplified in triplicates using the CS1-V3F(341) and CS2-V4R(515) primers (Table A.1). The samples were sequenced (2 x 150 bp) on the iSeq platform (Illumina, San Diego, CA, USA) at the Central and Northern Arava R&D Center (Israel).

2.5. Community analysis

Reads were merged, quality checked, and trimmed following the NeatSeq-Flow pipeline (Sklarz et al., 2018). The sequences were analysed using QIIME2 (Bolyen et al., 2018) and Dada2 (Callahan et al., 2016). Reads were clustered in amplicon sequence variants (ASVs) and taxonomy was assigned using Silva v138 (Quast et al., 2013). The total number of sequences can be found in Table A.2. All raw sequences used in this study can be found in BioProject (https://www.ncbi.nlm.nih.gov/ bioproject) under the submission number PRJNA718159.

2.6. Functional predictions

Functional predictions of the 16S amplicons was done using Piphillin (Iwai et al., 2016; Narayan et al., 2020) and the KEGG database with a 97%-identity cut-off (May 2020) (Kaneshisa and Goto, 2000). Steps of metabolic pathways for different methods of harvesting energy (organotrophy, lithotrophy and phototrophy) (Cordero et al., 2019; Greening et al., 2016; León-Sobrino et al., 2019; Tveit et al., 2019), for parts of the nitrogen cycle (Madigan et al., 2009), and for the survival of the individual during a drought (DNA conservation and repair, sporulation and Reactive Oxygen Species (ROS)-damage prevention) (Borisov et al.,

2013; Hansen et al., 2007; Henrikus et al., 2018; Preiss, 1984; Preiss and Sivak, 1999; Rajeev et al., 2013; Repar et al., 2012; Slade and Radman, 2011) were selected. Then, we picked out genes of interest from each step in the KEGG database and built our own database (Table A.3). The assignment of function to the KEGG numbers of the abundance table from Piphillin was done in R using phyloseq (McMurdie et al., 2017). The significance of temporal differences in predicted functionalities was evaluated using a non-parametric test (Kruskal-Wallis test and a post-hoc Dunn test (Dinno, 2017; Dunn, 1964; Kruskal and Wallis, 1952).

2.7. Statistical analysis

All statistical analysis was done using R (R Core Team, 2016) using the phyloseq (McMurdie et al., 2017) along with the ggplot2 (Wickham, 2016), vegan (Oksanen et al., 2014), magritt (Wickham and Bache, 2014), dplyr (Wickham et al., 2018), scales (Wickham, 2017), grid (Murrell, 2004) packages. The significance of difference between time points was determined using a non-parametric test: Kruskal-Wallis test and Dunn test (Dinno, 2017; Dunn, 1964; Kruskal and Wallis, 1952).

3. RESULTS

3.1. Temporal changes in the biocrust chlorophyll and chemical analyses

We have followed changes in the biocrust before, during and after a rain event and noted that a day after the rain (at T[1]) the biocrust in the sampling site was visibly greener than at any other sampling point (Figure 1). Following our observations, Figure 2 depicts the average chlorophyll concentrations along with the soil water content in the biocrust at each sampling point (Table A.4). The biocrust water content significantly increased between the dry season T[0] and the rain event T[R] (2.26% and 16.2%, respectively, $p = 0.05$; Table A.5). Then soil moisture significantly decreased to 3.67% at T[3] ($p < 0.05$). The chlorophyll concentrations significantly increased right after the rain event (from 8.45 mg chl/g soil to 14.57 mg chl/g soil, during the rain event, $p = 0.0002$; Table A.5), but decreased significantly in later days (from 14.57 mg chl/g to 11.17 mg chl/g soil, three days after the rain, $p > 0.02$; Table A.5). The total organic carbon (Figure A.1) and total nitrogen (Figure A.2) showed slight temporal changes (Table A.4) that were not significant (Table A.5).

3.2. Temporal changes in the microbial community composition

Figure 3 shows the bacterial community composition at the order level for each sampling point. The community is mostly composed of *Cyanobacteria, Actinobacteria*, and *Proteobacteria* (Figure 3; Table A.6). During the dry season, biocrust community composition differed significantly from the community depicted during the rain event (Table A.7). The differences were shown mostly in orders belonging to the *Actinobacteria* and *Cyanobacteria* phyla (Figure 3; $p < 0.05$, Table A.7). The relative abundance of *Cyanobacteria*, dominated by the *Cyanobacteriales*, increased during the rain event (from 22% to 41%, Table A.6; $p < 0.05$, Table A.7). While the relative abundance of *Actinobacteria*, dominated by *Micrococcales*, decreased during the rain event (from 50% to

206 19%, Table A.6; $p < 0.05$, Table A.7). In the days following the rain event, no major changes
207 were detected in the biocrust community (Figure 3; Table A.6 and A.7).
208
209 3.3. Temporal changes in the microbial function
210 Figure 4 shows the predicted function based on the taxonomic composition using Piphillin
211 (Iwai et al., 2016; Narayan et al., 2020). The values of the putative functional genes are
212 displayed in copy number (CN). The values were mostly lower in the dry season compared to
213 the hydration-desiccation cycle, except for light and energy sensing (Figure 4; Table A.8).
214 These differences were shown to be statistically significant ($p < 0.03$; Table A.9).
215

4. DISCUSSION

In the Negev Desert, biocrust bacterial communities were shown to alter during hydration. Most apparent was the change in the relative abundance of *Cyanobacteria* which increased while the abundance of *Actinobacteria* decreased (Figure 3) similar to results obtained under controlled conditions that hydrated the biocrust to saturation (Angel and Conrad, 2013). In another controlled experiment, the filamentous cyanobacterium *Leptolyngbya sp.* isolated from desert biocrust, was shown to respond quickly to both hydration and desiccation (Oren et al., 2019, 2017). Slight increase in biocrust moisture, triggered by dew simulation, induced DNA repair and associated regulatory genes for activating the photosynthetic system of the cyanobacterium (Murik et al., 2017; Rajeev et al., 2013). However, in this study we show that during a rain event of the Negev Desert biocrust, soil moisture increased and resulted in: (i) a sharp rise in chlorophyll concentrations (Figure 2), (ii) a significant increase in the relative abundance of various cyanobacterial orders (Figure 3; Table A.6 and A.7), and (iii) a significant increase in putative phototrophy of the community (Figure 4; Table A.8 and A.9). The concentration of the chlorophyll pigment was suggested to be linked to the water content (Péli et al., 2011) and to the activity of dominating primary producer in the biocrust, i.e., *Cyanobacteria* and/or green algae (Madigan et al., 2009). While cyanobacterial activity increased with soil moisture, no significant changes were detected in the total organic carbon and nitrogen content (Figure A.1 and A.2; Table A.4 and S5). This observation suggests that the immediate change in these parameters is negligible compared to existing soil reservoir; thus, it cannot be used as an indicator for the reaction of the local community to rain events. Moreover, it was recently proposed that in arid biocrusts, the dominant *Cyanobacteria* exchange carbon for nitrogen with copiotrophic diazotrophs, thus rapidly utilizing available nutrients and enabling the colonisation of the oligotrophic dryland soils (Couradeau et al., 2019).

241

242 In desert soil, rain events were shown to entail a decrease in the abundance of *Actinobacteria*
243 both in the biocrust (Angel and Conrad, 2013) and topsoil (Šťovíček et al., 2017). Members
244 of this phylum were shown to be well adapted to living in harsh environments (Goodfellow
245 and Williams, 1983; Zvyagintsev et al., 2007), and were found to be abundant in the Negev
246 Highland biocrust (Meier et al., 2021). Here we showed that the increase of water content
247 may lead to an increase in activity in all gene groups linked to energy usage or production
248 (Figure 4; Table A.8). The generally dry biocrust experiences a narrow window of hydration
249 conditions after a rain event of only a couple of days (Figure 2). These conditions are rapidly
250 exploited by phototrophs before the soil dries (Figure 2 and 3), and inhibit resilient
251 heterotrophs (Figure 3), as was previously shown in controlled (Cordero et al., 2019;
252 Greening et al., 2016; León-Sobrino et al., 2019; Tveit et al., 2019), and naturel (León-
253 Sobrino et al., 2019) settings.

254

255 We showed that re-hydration stage is quick and bacterial activity restarts within hours.
256 However, during the desiccation stage, changes are slower. The biocrust dries quickly after
257 the rain (Figure 2) due to evaporation, encouraged by the strong radiation, high winds, and
258 low air humidity (Kidron and Tal, 2012). Yet, unlike the response to dew hydration (Oren et
259 al., 2019, 2017), the community does not immediately inactivates. We sampled the soil along
260 the hydration-desiccation cycle and stopped sampling when the soil was dehydrated because
261 we expected inactivation of the community. In a previous study (Šťovíček et al., 2017), we
262 showed that the topsoil community bounces back to its original structure as soon as the soil
263 dries. Yet in the biocrust, dehydration was associated by a decrease in chlorophyll
264 concentrations, yet we detected no significant changes in the community composition (Figure
265 3). This may be possible due to the EPS produced by the *Cyanobacteria* (Mager and Thomas,

2011; Mazor et al., 1996) that dominate the biocrust. *Cyanobacteria* were shown to secrete copious amounts of EPS that bind the soil particles together (Kidron et al., 2020; Kidron and Tal, 2012). The EPS in the biocrust was shown to retain water in the soil, slowing down the drying process (Roberson and Firestone, 1992). Likewise, EPS in soil was shown to create microhabitats that retain humidity (Colica et al., 2014), thus stabilising the biocrust (Lan et al., 2012), and protecting the residing microorganisms from desiccation (Mazor et al., 1996). EPS is a key component in the Negev Desert biocrusts (Kidron et al., 2020). Here we propose that EPS may benefit the microbial community by creating microhabitats in which moisture is retained longer, enabling extended active phase following a rain event. This extra time to propagate after a rain event, may justify the ample resources invested by the *Cyanobacteria* in EPS production (Mager and Thomas, 2011). To validate this hypothesis further study is required.

5. CONCLUSION

In desert biocrusts, bacterial communities must respond quickly to hydration, in order to take advantage of the short windows of opportunity to photosynthesize, and then to desiccation to prevent cells damage. Our findings reinforce controlled studies showing that biocrust hydration change the bacterial community, increasing the *Cyanobacteria* abundance over *Actinobacteria*. However, here we have shown that under field conditions the response to soil desiccation is slower, allowing for a longer period of activity and production even a day after soil moisture decrease. we speculate that the lag in response to dehydration is due to EPS-based water retention in the soil mediated by the *Cyanobacteria* producers, justifying the metabolic cost of biocrust formation.

ACKNOWLEDGEMENT

The authors are grateful to Lusine Ghazaryan for technical support and to Ben Poodiack for editing the manuscript. This study was partially supported by the Israel Science Academy, grant no. 993/11.

297 REFERENCES

298 Aanderud, Z.T., Bahr, J., Robinson, D.M., Belnap, J., Campbell, T.P., Gill, R.A., McMillian,
299 B., St. Clair, S., 2019. The Burning of Biocrusts Facilitates the Emergence of a Bare Soil
300 Community of Poorly-Connected Chemoheterotrophic Bacteria With Depressed
301 Ecosystem Services. Front. Ecol. Evol. 7, 1–14. https://doi.org/10.3389/fevo.2019.00467
302 Agarwal, L., Qureshi, A., Kalia, V.C., Kapley, A., Purohit, H.J., Singh, R.N., 2014. Arid
303 ecosystem: Future option for carbon sinks using microbial community intelligence. Curr.
304 Sci. 106, 1357–1363.
305 Angel, R., 2012. Total Nucleic Acid Extraction from Soil.
306 Angel, R., Conrad, R., 2013. Elucidating the microbial resuscitation cascade in biological soil
307 crusts following a simulated rain event. Environ. Microbiol. 15, 2799–2815.
308 https://doi.org/10.1111/1462-2920.12140
309 Angel, R., Pasternak, Z., Soares, M.I.M., Conrad, R., Gillor, O., 2013. Active and total
310 prokaryotic communities in dryland soils. FEMS Microbiol. Ecol. 86, 130–138.
311 https://doi.org/10.1111/1574-6941.12155
312 Belnap, J., Lange, O.L., 2001. Biological Soil Crusts: Structure, Function, and Management,
313 Springer. https://doi.org/10.1639/0007-2745(2002)105[0500:]2.0.co;2
314 Bolyen, E., Rideout, J.R., Dillon, M.R., Bokulich, N.A., Abnet, C., Al-Ghalith, G.A.,
315 Alexander, H., Alm, E.J., Arumugam, M., Asnicar, F., Bai, Y., Bisanz, J.E., Bittinger,
316 K., Brejnrod, A., Brislawn, C.J., Brown, C.T., Callahan, B.J., Caraballo-Rodríguez,
317 A.M., Chase, J., Cope, E., Da Silva, R., Dorrestein, P.C., Douglas, G.M., Durall, D.M.,
318 Duvallet, C., Edwardson, C.F., Ernst, M., Estaki, M., Fouquier, J., Gauglitz, J.M.,
319 Gibson, D.L., Gonzalez, A., Gorlick, K., Guo, J., Hillmann, B., Holmes, S., Holste, H.,
320 Huttenhower, C., Huttley, G., Janssen, S., Jarmusch, A.K., Jiang, L., Kaehler, B., Kang,
321 K. Bin, Keefe, C.R., Keim, P., Kelley, S.T., Knights, D., Koester, I., Kosciolek, T.,

322 Kreps, J., Langille, M.G.I., Lee, J., Ley, R., Liu, Y.-X., Loftfield, E., Lozupone, C.,
323 Maher, M., Marotz, C., Martin, B.D., McDonald, D., McIver, L.J., Melnik, A. V,
324 Metcalf, J.L., Morgan, S.C., Morton, J., Naimey, A.T., Navas-Molina, J.A., Nothias,
325 L.F., Orchanian, S.B., Pearson, T., Peoples, S.L., Petras, D., Preuss, M.L., Pruesse, E.,
326 Rasmussen, L.B., Rivers, A., Robeson Michael S, I.I., Rosenthal, P., Segata, N., Shaffer,
327 M., Shiffer, A., Sinha, R., Song, S.J., Spear, J.R., Swafford, A.D., Thompson, L.R.,
328 Torres, P.J., Trinh, P., Tripathi, A., Turnbaugh, P.J., Ul-Hasan, S., van der Hooft, J.J.J.,
329 Vargas, F., Vázquez-Baeza, Y., Vogtmann, E., von Hippel, M., Walters, W., Wan, Y.,
330 Wang, M., Warren, J., Weber, K.C., Williamson, C.H.D., Willis, A.D., Xu, Z.Z.,
331 Zaneveld, J.R., Zhang, Y., Zhu, Q., Knight, R., Caporaso, J.G., 2018. QIIME 2:
332 Reproducible, interactive, scalable, and extensible microbiome data science. PeerJ Prepr.
333 6, e27295v2. https://doi.org/10.7287/peerj.preprints.27295v2
334 Borisov, V.B., Forte, E., Davletshin, A., Mastronicola, D., Sarti, P., Giuffrè, A., 2013.
335 Cytochrome bd oxidase from Escherichia coli displays high catalase activity: An
336 additional defense against oxidative stress. FEBS Lett. 587, 2214–2218.
337 https://doi.org/10.1016/j.febslet.2013.05.047
338 Bowker, M.A., Reed, S.C., Maestre, F.T., Eldridge, D.J., 2018. Biocrusts: the living skin of
339 the earth. Plant Soil 429, 1–7. https://doi.org/10.1007/s11104-018-3735-1
340 Callahan, B.J., McMurdie, P.J., Rosen, M.J., Han, A.W., Johnson, A.J.A., Holmes, S.P., 2016.
341 DADA2: High-resolution sample inference from Illumina amplicon data. Nat. Methods
342 13, 581–583. https://doi.org/10.1038/nmeth.3869
343 Cameron, R.E., Blank, G.B., 1966. Desert algae: soil crusts and diaphanous substrata as algal
344 habitats.
345 Campbell, S.E., Seeler, J., Golubic, S., 1989. Desert crust formation and soil stabilization.
346 Arid Soil Res. Rehabil. 3, 217–228. https://doi.org/10.1080/15324988909381200

347 Castillo-Monroy, A.P., Maestre, F.T., Rey, A., Soliveres, S., Garc??a-Palacios, P., 2011.
348 Biological Soil Crust Microsites Are the Main Contributor to Soil Respiration in a
349 Semiarid Ecosystem. Ecosystems 14, 835–847. https://doi.org/10.1007/s10021-011-
350 9449-3
351 Castle, S.C., Morrison, C.D., Barger, N.N., 2010. Extraction of chlorophyll a from biological
352 soil crusts: A comparison of solvents for spectrophotometric determination. Soil Biol.
353 Biochem. 43, 853–856. https://doi.org/10.1016/j.soilbio.2010.11.025
354 Colica, G., Li, H., Rossi, F., Li, D., Liu, Y., De Philippis, R., 2014. Microbial secreted
355 exopolysaccharides affect the hydrological behavior of induced biological soil crusts in
356 desert sandy soils. Soil Biol. Biochem. 68, 62–70.
357 https://doi.org/10.1016/j.soilbio.2013.09.017
358 Cordero, P.R.F., Bayly, K., Man Leung, P., Huang, C., Islam, Z.F., Schittenhelm, R.B., King,
359 G.M., Greening, C., 2019. Atmospheric carbon monoxide oxidation is a widespread
360 mechanism supporting microbial survival. ISME J. 13, 2868–2881.
361 https://doi.org/10.1038/s41396-019-0479-8
362 Couradeau, E., Giraldo-Silva, A., De Martini, F., Garcia-Pichel, F., 2019. Spatial segregation
363 of the biological soil crust microbiome around its foundational cyanobacterium,
364 Microcoleus vaginatus, and the formation of a nitrogen-fixing cyanosphere. Microbiome
365 7, 1–12. https://doi.org/10.1186/s40168-019-0661-2
366 Dinno, A., 2017. Package ‘dunn.test.’ CRAN Repos. 1–7.
367 Dunn, O.J., 1964. Multiple Comparisons Using Rank Sums. Technometrics 6, 241–252.
368 Goodfellow, M., Williams, S.T., 1983. Ecology of actinomycetes. Annu. Rev. Microbiol. 37,
369 189–216. https://doi.org/10.1146/annurev.mi.37.100183.001201
370 Greening, C., Biswas, A., Carere, C.R., Jackson, C.J., Taylor, M.C., Stott, M.B., Cook, G.M.,
371 Morales, S.E., 2016. Genomic and metagenomic surveys of hydrogenase distribution

372 indicate H 2 is a widely utilised energy source for microbial growth and survival. ISME
373 J. 10, 761–777. https://doi.org/10.1038/ismej.2015.153
374 Halverson, L.J., Jones, T.M., Firestone, M.K., 2000. Release of Intracellular Solutes by Four
375 Soil Bacteria Exposed to Dilution Stress. Soil Sci. Soc. Am. J. 64, 1630–1637.
376 https://doi.org/10.2136/sssaj2000.6451630x
377 Hansen, B.B., Henriksen, S., Aanes, R., Sæther, B.E., 2007. Ungulate impact on vegetation in
378 a two-level trophic system. Polar Biol. 30, 549–558. https://doi.org/10.1007/s00300-006-
379 0212-8
380 Harris, R.F., 1981. Effect of Water Potential on Microbial Growth and Activity. Water
381 Potential Relations Soil Microbiol., SSSA Special Publications.
382 https://doi.org/https://doi.org/10.2136/sssaspecpub9.c2
383 Henrikus, S.S., Wood, E.A., McDonald, J.P., Cox, M.M., Woodgate, R., Goodman, M.F., van
384 Oijen, A.M., Robinson, A., 2018. DNA polymerase IV primarily operates outside of
385 DNA replication forks in Escherichia coli. PLoS Genet. 14, 1–29.
386 https://doi.org/10.1371/journal.pgen.1007161
387 Hoogsteen, M.J.J., Lantinga, E.A., Bakker, E.J., Groot, J.C.J., Tittonell, P.A., 2015.
388 Estimating soil organic carbon through loss on ignition: Effects of ignition conditions
389 and structural water loss. Eur. J. Soil Sci. 66, 320–328.
390 https://doi.org/10.1111/ejss.12224
391 Iwai, S., Weinmaier, T., Schmidt, B.L., Albertson, D.G., Poloso, N.J., Dabbagh, K., DeSantis,
392 T.Z., 2016. Piphillin: Improved prediction of metagenomic content by direct inference
393 from human microbiomes. PLoS One 11, 1–18.
394 https://doi.org/10.1371/journal.pone.0166104
395 Kaneshisa, M., Goto, S., 2000. KEGG: Kyoto Encyclopedia of Genes and Genomes. Nucleic
396 Acids Res. 28, 27–30. https://doi.org/10.3892/ol.2020.11439

Kedem, I., Treves, H., Noble, G., Hagemann, M., Murik, O., Raanan, H., Oren, N., Giordano, M., Kaplan, A., 2020. Keep your friends close and your competitors closer: novel interspecies interaction in desert biological sand crusts. Phycologia 00, 1–8. https://doi.org/10.1080/00318884.2020.1843349

Kidron, G.J., Herrnstadt, I., Barzilay, E., 2002. The role of dew as a moisture source for sand microbiotic crusts in the Negev Desert, Israel. J. Arid Environ. 52, 517–533. https://doi.org/10.1006/jare.2002.1014

Kidron, G.J., Tal, S.Y., 2012. The effect of biocrusts on evaporation from sand dunes in the Negev Desert. Geoderma 179–180, 104–112. https://doi.org/10.1016/j.geoderma.2012.02.021

Kidron, G.J., Wang, Y., Herzberg, M., 2020. Exopolysaccharides may increase biocrust rigidity and induce runoff generation. J. Hydrol. 588, 125081. https://doi.org/10.1016/j.jhydrol.2020.125081

Klindworth, A., Pruesse, E., Schweer, T., Peplies, J., Quast, C., Horn, M., Glöckner, F.O., 2013. Evaluation of general 16S ribosomal RNA gene PCR primers for classical and next-generation sequencing-based diversity studies. Nucleic Acids Res. 41, 1–11. https://doi.org/10.1093/nar/gks808

Kruskal, W.H., Wallis, W.A., 1952. Use of Ranks in One-Criterion Variance Analysis. J. Am. Stat. Assoc. 47, 583–621. https://doi.org/10.1080/01621459.1952.10483441

Lan, S., Wu, L., Zhang, D., Hu, C., 2012. Successional stages of biological soil crusts and their microstructure variability in Shapotou region (China). Environ. Earth Sci. 65, 77–88. https://doi.org/10.1007/s12665-011-1066-0

Lennon, J.T., Jones, S.E., 2011. Microbial seed banks: The ecological and evolutionary implications of dormancy. Nat. Rev. Microbiol. 9, 119–130. https://doi.org/10.1038/nrmicro2504

León-Sobrino, C., Ramond, J.B., Maggs-Kölling, G., Cowan, D.A., 2019. Nutrient acquisition, rather than stress response over diel cycles, drives microbial transcription in a hyper-arid Namib desert soil. Front. Microbiol. 10, 1–11. https://doi.org/10.3389/fmicb.2019.01054

Leung, P.M., Bay, S.K., Meier, D. V., Chiri, E., Cowan, D.A., Gillor, O., Woebken, D., Greening, C., 2020. Energetic Basis of Microbial Growth and Persistence in Desert Ecosystems. mSystems 5, 1–14. https://doi.org/10.1128/msystems.00495-19

Madigan, M.T., Martinko, J.M., Dunlap, P. V, Clark, D.P., 2009. Brock Biology of microoragnisms.

Mager, D.M., Thomas, A.D., 2011. Extracellular polysaccharides from cyanobacterial soil crusts: A review of their role in dryland soil processes. J. Arid Environ. 75, 91–97. https://doi.org/10.1016/j.jaridenv.2010.10.001

Malek, E., McCurdy, G., Giles, B., 1999. Dew contribution to the annual water balances in semi-arid desert valleys. J. Arid Environ. 42, 71–80. https://doi.org/10.1006/jare.1999.0506

Mazor, G., Kidron, G.J., Vonshak, A., Abeliovich, A., 1996. The role of cyanobacterial exopolysaccharides in structuring desert microbial crusts. FEMS Microbiol. Ecol. 21, 121–130. https://doi.org/10.1016/0168-6496(96)00050-5

McMurdie, P.J., Holmes, S., Jordan, G., Chamberlain, S., 2017. Phyloseq: handling and analysis of high-throughput microbiome census data.

Meier, D. V., Imminger, S., Gillor, O., Woebken, D., 2021. Distribution of Mixotrophy and Desiccation Survival Mechanisms across Microbial Genomes in an Arid Biological Soil Crust Community. mSystems 6, 1–20. https://doi.org/10.1128/msystems.00786-20

Meier, D. V, Imminger, S., Gillor, O., Woebken, D., 2020. Versatility of energy metabolism and drought survival strategies characterize microbial genomes in biological soil crust.

Prep.

Murik, O., Oren, N., Shotland, Y., Raanan, H., Treves, H., Kedem, I., Keren, N., Hagemann, M., Pade, N., Kaplan, A., 2017. What distinguishes cyanobacteria able to revive after desiccation from those that cannot: the genome aspect. Environ. Microbiol. 19, 535–550. https://doi.org/10.1111/1462-2920.13486

Murrell, P., 2004. grid Graphics Creating and Controlling Graphics Regions and Co- ordinate Systems. Differences 1–17. https://doi.org/doi:10.1201/b10966-6

Narayan, N.R., Weinmaier, T., Laserna-Mendieta, E.J., Claesson, M.J., Shanahan, F., Dabbagh, K., Iwai, S., Desantis, T.Z., 2020. Piphillin predicts metagenomic composition and dynamics from DADA2- corrected 16S rDNA sequences. BMC Genomics 21, 1–12. https://doi.org/10.1186/s12864-020-6537-9

Oksanen, J., Blanchet, F.G., Kindt, R., Legen-, P., Minchin, P.R., Hara, R.B.O., Simpson, G.L., Solymos, P., Stevens, M.H.H., 2014. Package ‘ vegan .’ https://doi.org/ISBN 0-387-95457-0

Oren, N., Raanan, H., Kedem, I., Turjeman, A., Bronstein, M., Kaplan, A., Murik, O., 2019. Desert cyanobacteria prepare in advance for dehydration and rewetting: The role of light and temperature sensing. Mol. Ecol. 28, 2305–2320. https://doi.org/10.1111/mec.15074

Oren, N., Raanan, H., Murik, O., Keren, N., Kaplan, A., 2017. Dawn illumination prepares desert cyanobacteria for dehydration. Curr. Biol. 27, R1056–R1057. https://doi.org/10.1016/j.cub.2017.08.027

Péli, E.R., Lei, N., Pócs, T., Laufer, Z., Porembski, S., Tuba, Z., 2011. Ecophysiological responses of desiccation-tolerant cryptobiotic crusts. Cent. Eur. J. Biol. 6, 838–849. https://doi.org/10.2478/s11535-011-0049-1

Pointing, S.B., Belnap, J., 2012. Microbial colonization and controls in dryland systems. Nat. Rev. Microbiol. 10, 551–562. https://doi.org/10.1038/nrmicro2831

Preiss, J., 1984. Bacterial glycogen synthesis and its regulation. Annu. Rev. Microbiol. 38, 419–458.

Preiss, J., Sivak, M., 1999. 3.14 - Starch and Glycogen Biosynthesis, in: Barton, S.D., Nakanishi, K., Meth-Cohn, O.B.T.-C.N.P.C. (Eds.), . Pergamon, Oxford, pp. 441–495. https://doi.org/https://doi.org/10.1016/B978-0-08-091283-7.00082-5

Quast, C., Pruesse, E., Yilmaz, P., Gerken, J., Schweer, T., Yarza, P., Peplies, J., Glöckner, F.O., 2013. The SILVA ribosomal RNA gene database project: improved data processing and web-based tools. Nucleic Acids Res. 41, D590–D596. https://doi.org/10.1093/nar/gks1219

R Core Team, I., 2016. R: A language and environment for statistical computing [WWW Document]. R Found. Stat. Comput. URL http://www.r-project.org

Rajeev, L., Da Rocha, U.N., Klitgord, N., Luning, E.G., Fortney, J., Axen, S.D., Shih, P.M., Bouskill, N.J., Bowen, B.P., Kerfeld, C.A., Garcia-Pichel, F., Brodie, E.L., Northen, T.R., Mukhopadhyay, A., 2013. Dynamic cyanobacterial response to hydration and dehydration in a desert biological soil crust. ISME J. 7, 2178–2191. https://doi.org/10.1038/ismej.2013.83

Repar, J., Briski, N., Buljubašić, M., Zahradka, K., Zahradka, D., 2012. Exonuclease VII is involved in “reckless” DNA degradation in UV-irradiated Escherichia coli. Mutat. Res. 750. https://doi.org/10.1016/j.mrgentox.2012.10.005

Ritchie, R.J., 2006. Consistent sets of spectrophotometric chlorophyll equations for acetone, methanol and ethanol solvents. Photosynth. Res. 89, 27–41. https://doi.org/10.1007/s11120-006-9065-9

Roberson, E.B., Firestone, M.K., 1992. Relationship between desiccation and exopolysaccharide production in a soil Pseudomonas sp. Appl. Environ. Microbiol. 58, 1284–1291. https://doi.org/10.1128/aem.58.4.1284-1291.1992

497 Scrimgeour, C., 2008. Soil Sampling and Methods of Analysis (Second Edition),
498 Experimental Agriculture. https://doi.org/10.1017/s0014479708006546
499 Sklarz, M.Y., Levin, L., Gordon, M., Chalifa-Caspi, V., 2018. NeatSeq-Flow: A Lightweight
500 High Throughput Sequencing Workflow Platform for Non-Programmers and
501 Programmers alike. bioRxiv 173005. https://doi.org/10.1101/173005
502 Slade, D., Radman, M., 2011. Oxidative Stress Resistance in Deinococcus radiodurans,
503 Microbiology and Molecular Biology Reviews. https://doi.org/10.1128/mmbr.00015-10
504 Šťovíček, A., Kim, M., Or, D., Gillor, O., 2017. Microbial community response to hydration-
505 desiccation cycles in desert soil. Sci. Rep. 7, 45735. https://doi.org/10.1038/srep45735
506 Sukenik, A., Kaplan-Levy, R.N., Welch, J.M., Post, A.F., 2012. Massive multiplication of
507 genome and ribosomes in dormant cells (akinetes) of Aphanizomenon ovalisporum
508 (Cyanobacteria). ISME J. 6, 670–679. https://doi.org/10.1038/ismej.2011.128
509 Sunyer-Figueres, M., Wang, C., Mas, A., 2018. Analysis of ribosomal RNA stability in dead
510 cells of wine yeast by quantitative PCR. Int. J. Food Microbiol. 270, 1–4.
511 https://doi.org/10.1016/j.ijfoodmicro.2018.01.020
512 Tveit, A.T., Hestnes, A.G., Robinson, S.L., Schintlmeister, A., Dedysh, S.N., Jehmlich, N.,
513 Von Bergen, M., Herbold, C., Wagner, M., Richter, A., Svenning, M.M., 2019.
514 Widespread soil bacterium that oxidizes atmospheric methane. Proc. Natl. Acad. Sci. U.
515 S. A. 116, 8515–8524. https://doi.org/10.1073/pnas.1817812116
516 Wickham, H., 2017. R: Package 'scales.' Cran.
517 Wickham, H., 2016. Ggplot2: Elegant graphics for data analysis.
518 Wickham, H., Bache, S.M., 2014. Magrittr: A forward-pipe operator for R.
519 Wickham, H., Francois, R., Henry, L., Müller, K., 2018. Package "dplyr."
520 Wu, L., Lan, S., Zhang, D., Hu, C., 2013. Recovery of chlorophyll fluorescence and
521 CO2exchange in lichen soil crusts after rehydration. Eur. J. Soil Biol. 55, 77–82.

https://doi.org/10.1016/j.ejsobi.2012.12.006

Zvyagintsev, D.G., Zenova, G.M., Doroshenko, E.A., Gryadunova, A.A., Gracheva, T.A., Sudnitsyn, I.I., 2007. Actinomycete growth in conditions of low moisture. Biol. Bull. 34, 242–247. https://doi.org/10.1134/S1062359007030053

528 APPPENDIX A

529 Table A.1. Primers used in this study

530

	Primer name	Primers (5' – 3')	Reference
16S rRNA	V3F(341)	CCTACGGGAGGCAGCAG	(Klindworth et al., 2013)
	V4R(515)	TTACCGCGGCKGCTGGCAC	
	V4R(806)	GGACTACHVGGGTWTCTAAT	
Universal tags	CS1	ACACTGACGACATGGTTCTACA	
	CS2	TACGGTAGCAGAGACTTGGTCT	

531
532

533 Table A.2. Statistics from Dada2

Sample (Time point)	Input	Filtered	Percentage of input passed filter	Denoised	Non-chimeric	Percentage of input non-chimeric
T[R]	99090	87403	88.21	76272	68762	69.39
T[R]	102014	87207	85.49	75796	64954	63.67
T[R]	107763	94407	87.61	80242	72676	67.44
T[R]	94175	81352	86.38	69460	61519	65.32
T[R]	97752	85658	87.63	76694	65590	67.10
T[1]	102147	89670	87.79	79436	68611	67.17
T[1]	110406	96638	87.53	86745	76384	69.18
T[1]	94247	81576	86.56	72289	65755	69.77
T[1]	107731	94180	87.42	83504	72831	67.60
T[1]	96982	84993	87.64	77197	67547	69.65
T[2]	95525	82453	86.32	73811	63892	66.89
T[2]	90500	79303	87.63	75977	74636	82.47
T[2]	84648	74376	87.87	71060	69017	81.53
T[2]	96778	85143	87.98	75971	66483	68.70
T[2]	83749	72395	86.44	65649	60857	72.67
T[3]	85527	74977	87.66	66324	56872	66.50
T[3]	92648	81056	87.49	74512	67015	72.33
T[3]	98388	86526	87.94	78048	69910	71.06
T[3]	92219	79938	86.68	69799	62666	67.95
T[3]	88140	77515	87.95	73273	72113	81.82
T[0]	22095	21646	97.97	19900	12628	57.15
T[0]	23457	22888	97.57	18342	11627	49.57
T[0]	26072	25368	97.30	20726	12867	49.35

534
535

536 Table A.3. List of the genes used for function prediction ordered by groups and subgroups.

Group	Metabolic traits	KEGG ID	Function
DNA conservation	Putative DNA-binding protein	K02524	K10; DNA binding protein (fs(1)K10, female sterile(1)K10)
	Putative DNA-binding protein	K03111	ssb; single-strand DNA-binding protein
	Putative DNA-binding protein	K03530	hupB; DNA-binding protein HU-beta
	Putative DNA-binding protein	K03622	ssh10b; archaea-specific DNA-binding protein
	Putative DNA-binding protein	K03746	hns; DNA-binding protein H-NS
	Putative DNA-binding protein	K04047	dps; starvation-inducible DNA-binding protein
	Putative DNA-binding protein	K04494	CHD8, HELSNF1; chromodomain helicase DNA binding protein 8 [EC:3.6.4.12]
	Putative DNA-binding protein	K04680	ID1; DNA-binding protein inhibitor ID1
	Putative DNA-binding protein	K05516	cbpA; curved DNA-binding protein
	Putative DNA-binding protein	K05732	ARHGAP35, GRLF1; glucocorticoid receptor DNA-binding factor 1
	Putative DNA-binding protein	K05787	hupA; DNA-binding protein HU-alpha
	Putative DNA-binding protein	K09061	GCF, C2orf3; GC-rich sequence DNA-binding factor
	Putative DNA-binding protein	K09423	BAS1; Myb-like DNA-binding protein BAS1
	Putative DNA-binding protein	K09424	REB1; Myb-like DNA-binding protein REB1
	Putative DNA-binding protein	K09425	K09425; Myb-like DNA-binding protein FlbD
	Putative DNA-binding protein	K09426	RAP1; Myb-like DNA-binding protein RAP1

	Putative DNA-binding protein	K10140	DDB2; DNA damage-binding protein 2
	Putative DNA-binding protein	K10610	DDB1; DNA damage-binding protein 1
	Putative DNA-binding protein	K10728	TOPBP1; topoisomerase (DNA) II binding protein 1
	Putative DNA-binding protein	K10748	tus, tau; DNA replication terminus site-binding protein
	Histone-like protein	K10752	RBBP4, HAT2, CAF1, MIS16; histone-binding protein RBBP4
	Putative DNA-binding protein	K10979	ku; DNA end-binding protein Ku
	Putative DNA-binding protein	K11367	CHD1; chromodomain-helicase-DNA-binding protein 1 [EC:3.6.4.12]
	Histone-like protein	K11495	CENPA; histone H3-like centromeric protein A
	Putative DNA-binding protein	K11574	CBF2, CBF3A, CTF14; centromere DNA-binding protein complex CBF3 subunit A
	Putative DNA-binding protein	K11575	CEP3, CBF3B; centromere DNA-binding protein complex CBF3 subunit B
	Putative DNA-binding protein	K11576	CTF13, CBF3C; centromere DNA-binding protein complex CBF3 subunit C
	Putative DNA-binding protein	K11642	CHD3, MI2A; chromodomain-helicase-DNA-binding protein 3 [EC:3.6.4.12]
	Putative DNA-binding protein	K11643	CHD4, MI2B; chromodomain-helicase-DNA-binding protein 4 [EC:3.6.4.12]
	Histone-like protein	K11659	RBBP7; histone-binding protein RBBP7
	Putative DNA-binding protein	K11685	stpA; DNA-binding protein StpA
	Putative DNA-binding protein	K12965	ZBP1, DAI; Z-DNA binding protein 1
	Putative DNA-binding protein	K13102	KIN; DNA/RNA-binding protein KIN17
	Putative DNA-binding protein	K13211	GCFC; GC-rich sequence DNA-binding factor
	Putative DNA-binding protein	K14435	CHD5; chromodomain-helicase-DNA-binding protein 5 [EC:3.6.4.12]

	Putative DNA-binding protein	K14436	CHD6; chromodomain-helicase-DNA-binding protein 6 [EC:3.6.4.12]
	Putative DNA-binding protein	K14437	CHD7; chromodomain-helicase-DNA-binding protein 7 [EC:3.6.4.12]
	Putative DNA-binding protein	K14438	CHD9; chromodomain-helicase-DNA-binding protein 9 [EC:3.6.4.12]
	Putative DNA-binding protein	K14507	ORCA2_3; AP2-domain DNA-binding protein ORCA2/3
	Histone-like protein	K15719	NCOAT, MGEA5; protein O-GlcNAcase / histone acetyltransferase [EC:3.2.1.169 2.3.1.48]
	Putative DNA-binding protein	K16640	ssh7; DNA-binding protein 7 [EC:3.1.27.-]
	Putative DNA-binding protein	K17693	ID2; DNA-binding protein inhibitor ID2
	Putative DNA-binding protein	K17694	ID3; DNA-binding protein inhibitor ID3
	Putative DNA-binding protein	K17695	ID4; DNA-binding protein inhibitor ID4
	Putative DNA-binding protein	K17696	EMC; DNA-binding protein inhibitor ID, other
	Histone-like protein	K18710	SLBP; histone RNA hairpin-binding protein
	Putative DNA-binding protein	K18946	gp32, ssb; single-stranded DNA-binding protein
	Putative DNA-binding protein	K19442	ICP8, DBP, UL29; Simplexvirus major DNA-binding protein
	Histone-like protein	K19799	RPH1; DNA damage-responsive transcriptional repressor / [histone H3]-trimethyl-L-lysine36 demethylase [EC:1.14.11.69]
	Putative DNA-binding protein	K20091	CHD2; chromodomain-helicase-DNA-binding protein 2 [EC:3.6.4.12]
	Putative DNA-binding protein	K20092	CHD1L; chromodomain-helicase-DNA-binding protein 1-like [EC:3.6.4.12]
	Putative DNA-binding protein	K22592	AHDC1; AT-hook DNA-binding motif-containing protein 1
	Putative DNA-binding protein	K23225	SATB1; DNA-binding protein SATB1
	Putative DNA-binding	K23226	SATB2; DNA-binding protein SATB2

	protein		
	Putative DNA-binding protein	K23600	TARDBP, TDP43; TAR DNA-binding protein 43
DNA repair	DNA polymerase PolA (COG0258)	K02320	POLA1; DNA polymerase alpha subunit A [EC:2.7.7.7]
	DNA polymerase PolA (COG0258)	K02321	POLA2; DNA polymerase alpha subunit B
	DNA polymerase PolA (COG0258)	K02335	polA; DNA polymerase I [EC:2.7.7.7]
	DNA polymerase IV	K02346	dinB; DNA polymerase IV [EC:2.7.7.7]
	Exodeoxyribonuclease VII	K03601	xseA; exodeoxyribonuclease VII large subunit [EC:3.1.11.6]
	Exodeoxyribonuclease VII	K03602	xseB; exodeoxyribonuclease VII small subunit [EC:3.1.11.6]
	DNA polymerase IV	K04479	dbh; DNA polymerase IV (archaeal DinB-like DNA polymerase) [EC:2.7.7.7]
	Exodeoxyribonuclease VII	K10906	recE; exodeoxyribonuclease VIII [EC:3.1.11.-]
	DNA polymerase IV	K10981	POL4; DNA polymerase IV [EC:2.7.7.7]
	DNA polymerase IV	K16250	NRPD1; DNA-directed RNA polymerase IV subunit 1 [EC:2.7.7.6]
	DNA polymerase IV	K16252	NRPD2, NRPE2; DNA-directed RNA polymerase IV and V subunit 2 [EC:2.7.7.6]
	DNA polymerase IV	K16253	NRPD7, NRPE7; DNA-directed RNA polymerase IV and V subunit 7
Litotrophy	NiFe hydrogenase	K00437	hydB; [NiFe] hydrogenase large subunit [EC:1.12.2.1]
	NiFe hydrogenase	K02587	nifE; nitrogenase molybdenum-cofactor synthesis protein NifE
	CO-dehydrogenase CoxM & CoxS	K03518	coxS; aerobic carbon-monoxide dehydrogenase small subunit [EC:1.2.5.3]
	CO-dehydrogenase CoxM & CoxS	K03519	coxM, cutM; aerobic carbon-monoxide dehydrogenase medium subunit [EC:1.2.5.3]
	CO-dehydrogenase large subunit (coxL) Form I	K03520	coxL, cutL; aerobic carbon-monoxide dehydrogenase large subunit [EC:1.2.5.3]
	NiFe hydrogenase	K05586	hoxE; bidirectional [NiFe] hydrogenase diaphorase subunit [EC:7.1.1.2]
	NiFe hydrogenase	K05587	hoxF; bidirectional [NiFe] hydrogenase diaphorase subunit [EC:7.1.1.2]
	NiFe hydrogenase	K05588	hoxU; bidirectional [NiFe] hydrogenase diaphorase subunit [EC:7.1.1.2]

	SOX sulfur-oxidation system	K17218	sqr; sulfide:quinone oxidoreductase [EC:1.8.5.4]
	SOX sulfur-oxidation system	K17222	soxA; L-cysteine S-thiosulfotransferase [EC:2.8.5.2]
	SOX sulfur-oxidation system	K17223	soxX; L-cysteine S-thiosulfotransferase [EC:2.8.5.2]
	SOX sulfur-oxidation system	K17224	soxB; S-sulfosulfanyl-L-cysteine sulfohydrolase [EC:3.1.6.20]
	SOX sulfur-oxidation system	K17225	soxC; sulfane dehydrogenase subunit SoxC
	SOX sulfur-oxidation system	K17226	soxY; sulfur-oxidizing protein SoxY
	SOX sulfur-oxidation system	K17227	soxZ; sulfur-oxidizing protein SoxZ
	NiFe hydrogenase	K18005	hoxF; [NiFe] hydrogenase diaphorase moiety large subunit [EC:1.12.1.2]
	NiFe hydrogenase	K18006	hoxU; [NiFe] hydrogenase diaphorase moiety small subunit [EC:1.12.1.2]
	NiFe hydrogenase	K18008	hydA; [NiFe] hydrogenase small subunit [EC:1.12.2.1]
	Propane monooxygenase (soluble)	K18223	prmA; propane 2-monooxygenase large subunit [EC:1.14.13.227]
	Propane monooxygenase (soluble)	K18224	prmC; propane 2-monooxygenase small subunit [EC:1.14.13.227]
	Propane monooxygenase (soluble)	K18225	prmB; propane monooxygenase reductase component [EC:1.18.1.-]
	Propane monooxygenase (soluble)	K18226	prmD; propane monooxygenase coupling protein
	SOX sulfur-oxidation system	K22622	soxD; S-disulfanyl-L-cysteine oxidoreductase SoxD [EC:1.8.2.6]
	SOX sulfur-oxidation system	K24007	soxD; cytochrome aa3-type oxidase subunit SoxD
	SOX sulfur-oxidation system	K24008	soxC; cytochrome aa3-type oxidase subunit III
	SOX sulfur-oxidation system	K24009	soxB; cytochrome aa3-type oxidase subunit I [EC:7.1.1.4]
	SOX sulfur-oxidation system	K24010	soxA; cytochrome aa3-type oxidase subunit II [EC:7.1.1.4]

	SOX sulfur-oxidation system	K24011	soxM; cytochrome aa3-type oxidase subunit I/III [EC:7.1.1.4]
Organotrophy	ABC sugar transporters	K02025	ABC.MS.P; multiple sugar transport system permease protein
	ABC sugar transporters	K02026	ABC.MS.P1; multiple sugar transport system permease protein
	ABC sugar transporters	K02027	ABC.MS.S; multiple sugar transport system substrate-binding protein
	ABC sugar transporters	K02056	ABC.SS.A; simple sugar transport system ATP-binding protein [EC:7.5.2.-]
	ABC sugar transporters	K02057	ABC.SS.P; simple sugar transport system permease protein
	ABC sugar transporters	K02058	ABC.SS.S; simple sugar transport system substrate-binding protein
	PTS sugar importers	K02777	crr; sugar PTS system EIIA component [EC:2.7.1.-]
	Amino acid transporter	K03293	TC.AAT; amino acid transporter, AAT family
	Peptide transporter	K03305	TC.POT; proton-dependent oligopeptide transporter, POT family
	Amino acid transporter	K03311	TC.LIVCS; branched-chain amino acid:cation transporter, LIVCS family
	Carboxylate transporters	K03326	TC.DCUC, dcuC, dcuD; C4-dicarboxylate transporter, DcuC family
	Amino acid transporter	K03450	SLC7A; solute carrier family 7 (L-type amino acid transporter), other
	Glycosyl hydrolases	K04844	ycjT; hypothetical glycosyl hydrolase [EC:3.2.1.-]
	Amino acid transporter	K05048	SLC6A15S; solute carrier family 6 (neurotransmitter transporter, amino acid/orphan) member 15/16/17/18/20
	Amino acid transporter	K05615	SLC1A4, SATT; solute carrier family 1 (neutral amino acid transporter), member 4
	Amino acid transporter	K05616	SLC1A5; solute carrier family 1 (neutral amino acid transporter), member 5
	Amino acid transporter	K07084	yuiF; putative amino acid transporter
	Carboxylate transporters	K07791	dcuA; anaerobic C4-dicarboxylate transporter DcuA
	Carboxylate transporters	K07792	dcuB; anaerobic C4-dicarboxylate transporter DcuB
	ABC sugar transporters	K10546	ABC.GGU.S, chvE; putative multiple sugar transport system substrate-binding protein
	ABC sugar transporters	K10547	ABC.GGU.P, gguB; putative multiple sugar transport system permease protein
	ABC sugar transporters	K10548	ABC.GGU.A, gguA; putative multiple sugar transport system ATP-binding protein [EC:7.5.2.-]
	Carboxylate transporters	K11689	dctQ; C4-dicarboxylate transporter, DctQ subunit
	Carboxylate transporters	K11690	dctM; C4-dicarboxylate transporter, DctM subunit
	Amino acid transporter	K13576	SLC38A3, SNAT3; solute carrier family 38 (sodium-coupled neutral amino acid transporter), member 3

	Carboxylate transporters	K13577	SLC25A10, DIC; solute carrier family 25 (mitochondrial dicarboxylate transporter), member 10
	Amino acid transporter	K13780	SLC7A5, LAT1; solute carrier family 7 (L-type amino acid transporter), member 5
	Amino acid transporter	K13781	SLC7A8, LAT2; solute carrier family 7 (L-type amino acid transporter), member 8
	Amino acid transporter	K13782	SLC7A10, ASC1; solute carrier family 7 (L-type amino acid transporter), member 10
	Amino acid transporter	K13863	SLC7A1, ATRC1; solute carrier family 7 (cationic amino acid transporter), member 1
	Amino acid transporter	K13864	SLC7A2, ATRC2; solute carrier family 7 (cationic amino acid transporter), member 2
	Amino acid transporter	K13865	SLC7A3, ATRC3; solute carrier family 7 (cationic amino acid transporter), member 3
	Amino acid transporter	K13866	SLC7A4; solute carrier family 7 (cationic amino acid transporter), member 4
	Amino acid transporter	K13867	SLC7A7; solute carrier family 7 (L-type amino acid transporter), member 7
	Amino acid transporter	K13868	SLC7A9, BAT1; solute carrier family 7 (L-type amino acid transporter), member 9
	Amino acid transporter	K13869	SLC7A11; solute carrier family 7 (L-type amino acid transporter), member 11
	Amino acid transporter	K13870	SLC7A13, AGT1; solute carrier family 7 (L-type amino acid transporter), member 13
	Amino acid transporter	K13871	SLC7A14; solute carrier family 7 (cationic amino acid transporter), member 14
	Amino acid transporter	K13872	SLC7A6; solute carrier family 7 (L-type amino acid transporter), member 6
	Peptide transporter	K14206	SLC15A1, PEPT1; solute carrier family 15 (oligopeptide transporter), member 1
	Amino acid transporter	K14207	SLC38A2, SNAT2; solute carrier family 38 (sodium-coupled neutral amino acid transporter), member 2
	Amino acid transporter	K14209	SLC36A, PAT; solute carrier family 36 (proton-coupled amino acid transporter)
	Amino acid transporter	K14210	SLC3A1, RBAT; solute carrier family 3 (neutral and basic amino acid transporter), member 1
	Carboxylate transporters	K14388	SLC5A8_12, SMCT; solute carrier family 5 (sodium-coupled monocarboxylate transporter), member 8/12
	Carboxylate transporters	K14445	SLC13A2_3_5; solute carrier family 13 (sodium-dependent dicarboxylate transporter), member 2/3/5
	Peptide transporter	K14637	SLC15A2, PEPT2; solute carrier family 15 (oligopeptide transporter), member 2
	Peptide transporter	K14638	SLC15A3_4, PHT; solute carrier family 15 (peptide/histidine transporter), member 3/4
	Amino acid transporter	K14990	SLC38A1, SNAT1, GLNT; solute carrier family 38 (sodium-coupled neutral amino acid transporter), member 1
	Amino acid transporter	K14991	SLC38A4, SNAT4; solute carrier family 38 (sodium-coupled neutral amino acid transporter), member 4
	Amino acid transporter	K14992	SLC38A5, SNAT5; solute carrier family 38 (sodium-coupled neutral amino acid transporter), member 5
	Amino acid transporter	K14993	SLC38A6, SNAT6; solute carrier family 38 (sodium-coupled neutral amino acid transporter), member 6
	Amino acid	K14	SLC38A7_8; solute carrier family 38 (sodium-coupled

	transporter	994	neutral amino acid transporter), member 7/8
	Amino acid transporter	K14995	SLC38A9; solute carrier family 38 (sodium-coupled neutral amino acid transporter), member 9
	Amino acid transporter	K14996	SLC38A10; solute carrier family 38 (sodium-coupled neutral amino acid transporter), member 10
	Amino acid transporter	K14997	SLC38A11; solute carrier family 38 (sodium-coupled neutral amino acid transporter), member 11
	Amino acid transporter	K15015	SLC32A, VGAT; solute carrier family 32 (vesicular inhibitory amino acid transporter)
	Carboxylate transporters	K15110	SLC25A21, ODC; solute carrier family 25 (mitochondrial 2-oxodicarboxylate transporter), member 21
	Amino acid transporter	K16261	YAT; yeast amino acid transporter
	Amino acid transporter	K16263	yjeH; amino acid efflux transporter
	Peptide transporter	K17938	sbmA, bacA; peptide/bleomycin uptake transporter
Photothrophy	RuBisCO	K01601	rbcL; ribulose-bisphosphate carboxylase large chain [EC:4.1.1.39]
	Chlorophyll synthesis	K01669	phrB; deoxyribodipyrimidine photo-lyase [EC:4.1.99.3]
	Chlorophyll synthesis	K02689	psaA; photosystem I P700 chlorophyll a apoprotein A1
	Chlorophyll synthesis	K02690	psaB; photosystem I P700 chlorophyll a apoprotein A2
	Chlorophyll synthesis	K02691	psaC; photosystem I subunit VII
	Chlorophyll synthesis	K02692	psaD; photosystem I subunit II
	Chlorophyll synthesis	K02693	psaE; photosystem I subunit IV
	Chlorophyll synthesis	K02694	psaF; photosystem I subunit III
	Chlorophyll synthesis	K02695	psaH; photosystem I subunit VI
	Chlorophyll synthesis	K02696	psaI; photosystem I subunit VIII
	Chlorophyll synthesis	K02697	psaJ; photosystem I subunit IX
	Chlorophyll synthesis	K02698	psaK; photosystem I subunit X
	Chlorophyll synthesis	K02699	psaL; photosystem I subunit XI
	Chlorophyll synthesis	K02700	psaM; photosystem I subunit XII
	Chlorophyll synthesis	K02701	psaN; photosystem I subunit PsaN
	Chlorophyll synthesis	K02702	psaX; photosystem I 4.8kDa protein
	Chlorophyll synthesis	K02703	psbA; photosystem II P680 reaction center D1 protein [EC:1.10.3.9]
	Chlorophyll	K02	psbB; photosystem II CP47 chlorophyll apoprotein

	synthesis	704	
	Chlorophyll synthesis	K02 705	psbC; photosystem II CP43 chlorophyll apoprotein
	Chlorophyll synthesis	K02 706	psbD; photosystem II P680 reaction center D2 protein [EC:1.10.3.9]
	Chlorophyll synthesis	K02 707	psbE; photosystem II cytochrome b559 subunit alpha
	Chlorophyll synthesis	K02 708	psbF; photosystem II cytochrome b559 subunit beta
	Chlorophyll synthesis	K02 709	psbH; photosystem II PsbH protein
	Chlorophyll synthesis	K02 710	psbI; photosystem II PsbI protein
	Chlorophyll synthesis	K02 711	psbJ; photosystem II PsbJ protein
	Chlorophyll synthesis	K02 712	psbK; photosystem II PsbK protein
	Chlorophyll synthesis	K02 713	psbL; photosystem II PsbL protein
	Chlorophyll synthesis	K02 714	psbM; photosystem II PsbM protein
	Chlorophyll synthesis	K02 716	psbO; photosystem II oxygen-evolving enhancer protein 1
	Chlorophyll synthesis	K02 717	psbP; photosystem II oxygen-evolving enhancer protein 2
	Chlorophyll synthesis	K02 718	psbT; photosystem II PsbT protein
	Chlorophyll synthesis	K02 719	psbU; photosystem II PsbU protein
	Chlorophyll synthesis	K02 720	psbV; photosystem II cytochrome c550
	Chlorophyll synthesis	K02 721	psbW; photosystem II PsbW protein
	Chlorophyll synthesis	K02 722	psbX; photosystem II PsbX protein
	Chlorophyll synthesis	K02 723	psbY; photosystem II PsbY protein
	Chlorophyll synthesis	K02 724	psbZ; photosystem II PsbZ protein
	Chlorophyll synthesis	K03 157	LTB, TNFC; lymphotoxin beta (TNF superfamily, member 3)
	Chlorophyll synthesis	K03 159	TNFRSF3, LTBR; lymphotoxin beta receptor TNFR superfamily member 3
	Chlorophyll synthesis	K03 541	psbR; photosystem II 10kDa protein
	Chlorophyll synthesis	K03 542	psbS; photosystem II 22kDa protein
	Chlorophyll synthesis	K03 716	splB; spore photoproduct lyase [EC:4.1.99.14]
	Chlorophyll synthesis	K05 468	LTA, TNFB; lymphotoxin alpha (TNF superfamily, member 1)
	Chlorophyll synthesis	K06 315	splA; transcriptional regulator of the spore photoproduct lyase operon

	Chlorophyll synthesis	K06876	K06876; deoxyribodipyrimidine photolyase-related protein
	Chlorophyll synthesis	K08901	psbQ; photosystem II oxygen-evolving enhancer protein 3
	Chlorophyll synthesis	K08902	psb27; photosystem II Psb27 protein
	Chlorophyll synthesis	K08903	psb28; photosystem II 13kDa protein
	Chlorophyll synthesis	K08904	psb28-2; photosystem II Psb28-2 protein
	Chlorophyll synthesis	K08905	psaG; photosystem I subunit V
	Chlorophyll synthesis	K08928	pufL; photosynthetic reaction center L subunit
	Chlorophyll synthesis	K08929	pufM; photosynthetic reaction center M subunit
	Chlorophyll synthesis	K08940	pscA; photosystem P840 reaction center large subunit
	Chlorophyll synthesis	K08941	pscB; photosystem P840 reaction center iron-sulfur protein
	Chlorophyll synthesis	K08942	pscC; photosystem P840 reaction center cytochrome c551
	Chlorophyll synthesis	K08943	pscD; photosystem P840 reaction center protein PscD
	Chlorophyll synthesis	K11524	pixI; positive phototaxis protein PixI
	Chlorophyll synthesis	K13991	puhA; photosynthetic reaction center H subunit
	Chlorophyll synthesis	K13992	pufC; photosynthetic reaction center cytochrome c subunit
	Chlorophyll synthesis	K13994	pufX; photosynthetic reaction center PufX protein
	Chlorophyll synthesis	K14332	psaO; photosystem I subunit PsaO
	Chlorophyll synthesis	K19016	IMPG1, SPACR; interphotoreceptor matrix proteoglycan 1
	Chlorophyll synthesis	K19017	IMPG2, SPACRCAN; interphotoreceptor matrix proteoglycan 2
	Chlorophyll synthesis	K20715	PHOT; phototropin [EC:2.7.11.1]
	Chlorophyll synthesis	K22464	FAP; fatty acid photodecarboxylase [EC:4.1.1.106]
	Chlorophyll synthesis	K22619	Aequorin; calcium-regulated photoprotein [EC:1.13.12.24]
	Chlorophyll synthesis	K24165	PCARE; photoreceptor cilium actin regulator
ROS-damage prevention	Cytochrome C oxidase	K00404	ccoN; cytochrome c oxidase cbb3-type subunit I [EC:7.1.1.9]
	Cytochrome C oxidase	K00405	ccoO; cytochrome c oxidase cbb3-type subunit II
	Cytochrome C oxidase	K00406	ccoP; cytochrome c oxidase cbb3-type subunit III
	Cytochrome C oxidase	K00407	ccoQ; cytochrome c oxidase cbb3-type subunit IV

	Cytochrome bd ubiquinol oxidase	K00424	cydX; cytochrome bd-I ubiquinol oxidase subunit X [EC:7.1.1.7]
	Cytochrome C oxidase	K00424	cydX; cytochrome bd-I ubiquinol oxidase subunit X [EC:7.1.1.7]
	Cytochrome bd ubiquinol oxidase	K00425	cydA; cytochrome bd ubiquinol oxidase subunit I [EC:7.1.1.7]
	Cytochrome C oxidase	K00425	cydA; cytochrome bd ubiquinol oxidase subunit I [EC:7.1.1.7]
	Cytochrome bd ubiquinol oxidase	K00426	cydB; cytochrome bd ubiquinol oxidase subunit II [EC:7.1.1.7]
	Cytochrome C oxidase	K00426	cydB; cytochrome bd ubiquinol oxidase subunit II [EC:7.1.1.7]
	Cytochrome C oxidase	K00428	E1.11.1.5; cytochrome c peroxidase [EC:1.11.1.5]
	Cytochrome C oxidase	K02256	COX1; cytochrome c oxidase subunit 1 [EC:7.1.1.9]
	Cytochrome C oxidase	K02258	COX11, ctaG; cytochrome c oxidase assembly protein subunit 11
	Cytochrome C oxidase	K02259	COX15, ctaA; cytochrome c oxidase assembly protein subunit 15
	Cytochrome C oxidase	K02260	COX17; cytochrome c oxidase assembly protein subunit 17
	Cytochrome C oxidase	K02261	COX2; cytochrome c oxidase subunit 2
	Cytochrome C oxidase	K02262	COX3; cytochrome c oxidase subunit 3
	Cytochrome C oxidase	K02263	COX4; cytochrome c oxidase subunit 4
	Cytochrome C oxidase	K02264	COX5A; cytochrome c oxidase subunit 5a
	Cytochrome C oxidase	K02265	COX5B; cytochrome c oxidase subunit 5b
	Cytochrome C oxidase	K02266	COX6A; cytochrome c oxidase subunit 6a
	Cytochrome C oxidase	K02267	COX6B; cytochrome c oxidase subunit 6b
	Cytochrome C oxidase	K02268	COX6C; cytochrome c oxidase subunit 6c
	Cytochrome C oxidase	K02269	COX7; cytochrome c oxidase subunit 7
	Cytochrome C oxidase	K02270	COX7A; cytochrome c oxidase subunit 7a
	Cytochrome C oxidase	K02271	COX7B; cytochrome c oxidase subunit 7b
	Cytochrome C oxidase	K02272	COX7C; cytochrome c oxidase subunit 7c
	Cytochrome C oxidase	K02273	COX8; cytochrome c oxidase subunit 8
	Cytochrome C oxidase	K02274	coxA, ctaD; cytochrome c oxidase subunit I [EC:7.1.1.9]
	Cytochrome C	K02	coxB, ctaC; cytochrome c oxidase subunit II

	oxidase	275	[EC:7.1.1.9]
	Cytochrome C oxidase	K02276	coxC, ctaE; cytochrome c oxidase subunit III [EC:7.1.1.9]
	Cytochrome C oxidase	K02277	coxD, ctaF; cytochrome c oxidase subunit IV [EC:7.1.1.9]
	Cytochrome C oxidase	K02297	cyoA; cytochrome o ubiquinol oxidase subunit II [EC:7.1.1.3]
	Cytochrome C oxidase	K02298	cyoB; cytochrome o ubiquinol oxidase subunit I [EC:7.1.1.3]
	Cytochrome C oxidase	K02299	cyoC; cytochrome o ubiquinol oxidase subunit III
	Cytochrome C oxidase	K02300	cyoD; cytochrome o ubiquinol oxidase subunit IV
	Cytochrome C oxidase	K02826	qoxA; cytochrome aa3-600 menaquinol oxidase subunit II [EC:7.1.1.5]
	Cytochrome C oxidase	K02827	qoxB; cytochrome aa3-600 menaquinol oxidase subunit I [EC:7.1.1.5]
	Cytochrome C oxidase	K02828	qoxC; cytochrome aa3-600 menaquinol oxidase subunit III [EC:7.1.1.5]
	Cytochrome C oxidase	K02829	qoxD; cytochrome aa3-600 menaquinol oxidase subunit IV [EC:7.1.1.5]
	Mn2+ catalase	K07217	K07217; Mn-containing catalase
	Cytochrome C oxidase	K15408	coxAC; cytochrome c oxidase subunit I+III [EC:7.1.1.9]
	Cytochrome C oxidase	K15862	ccoNO; cytochrome c oxidase cbb3-type subunit I/II [EC:7.1.1.9]
	Cytochrome C oxidase	K18173	COA1; cytochrome c oxidase assembly factor 1
	Cytochrome C oxidase	K18174	COA2; cytochrome c oxidase assembly factor 2
	Cytochrome C oxidase	K18175	CCDC56, COA3; cytochrome c oxidase assembly factor 3, animal type
	Cytochrome C oxidase	K18176	COA3; cytochrome c oxidase assembly factor 3, fungi type
	Cytochrome C oxidase	K18177	COA4; cytochrome c oxidase assembly factor 4
	Cytochrome C oxidase	K18178	COA5, PET191; cytochrome c oxidase assembly factor 5
	Cytochrome C oxidase	K18179	COA6; cytochrome c oxidase assembly factor 6
	Cytochrome C oxidase	K18180	COA7, SELRC1, RESA1; cytochrome c oxidase assembly factor 7
	Cytochrome C oxidase	K18181	COX14; cytochrome c oxidase assembly factor 14
	Cytochrome C oxidase	K18182	COX16; cytochrome c oxidase assembly protein subunit 16
	Cytochrome C oxidase	K18183	COX19; cytochrome c oxidase assembly protein subunit 19
	Cytochrome C oxidase	K18184	COX20; cytochrome c oxidase assembly protein subunit 20
	Cytochrome C oxidase	K18185	COX23; cytochrome c oxidase assembly protein subunit 23

	Cytochrome C oxidase	K18189	TACO1; translational activator of cytochrome c oxidase 1
	Cytochrome bd ubiquinol oxidase	K22501	appX; cytochrome bd-II ubiquinol oxidase subunit AppX [EC:7.1.1.7]
	Cytochrome C oxidase	K22501	appX; cytochrome bd-II ubiquinol oxidase subunit AppX [EC:7.1.1.7]
	Cytochrome C oxidase	K24007	soxD; cytochrome aa3-type oxidase subunit SoxD
	Cytochrome C oxidase	K24008	soxC; cytochrome aa3-type oxidase subunit III
	Cytochrome C oxidase	K24009	soxB; cytochrome aa3-type oxidase subunit I [EC:7.1.1.4]
	Cytochrome C oxidase	K24010	soxA; cytochrome aa3-type oxidase subunit II [EC:7.1.1.4]
	Cytochrome C oxidase	K24011	soxM; cytochrome aa3-type oxidase subunit I/III [EC:7.1.1.4]
Sporulation	Glycogen synthesis	K00693	GYS; glycogen synthase [EC:2.4.1.11]
	Sporulation (Actinobacteria)	K02490	spo0F; two-component system, response regulator, stage 0 sporulation protein F
	Sporulation (Actinobacteria)	K02491	kinA; two-component system, sporulation sensor kinase A [EC:2.7.13.3]
	Glycogen synthesis	K03083	GSK3B; glycogen synthase kinase 3 beta [EC:2.7.11.26]
	Sporulation (Actinobacteria)	K03091	sigH; RNA polymerase sporulation-specific sigma factor
	Sporulation (Actinobacteria)	K04769	spoVT; AbrB family transcriptional regulator, stage V sporulation protein T
	Sporulation (Actinobacteria)	K06283	spoIIID; putative DeoR family transcriptional regulator, stage III sporulation protein D
	Sporulation (Actinobacteria)	K06348	kapD; sporulation inhibitor KapD
	Sporulation (Actinobacteria)	K06359	rapA, spo0L; response regulator aspartate phosphatase A (stage 0 sporulation protein L) [EC:3.1.-.-]
	Sporulation (Actinobacteria)	K06371	sda; developmental checkpoint coupling sporulation initiation to replication initiation
	Sporulation (Actinobacteria)	K06375	spo0B; stage 0 sporulation protein B (sporulation initiation phosphotransferase) [EC:2.7.-.-]
	Sporulation (Actinobacteria)	K06376	spo0E; stage 0 sporulation regulatory protein
	Sporulation (Actinobacteria)	K06377	spo0M; sporulation-barren protein

	Sporulation (Actinobacteria)	K06378	spoIIAA; stage II sporulation protein AA (anti-sigma F factor antagonist)
	Sporulation (Actinobacteria)	K06379	spoIIAB; stage II sporulation protein AB (anti-sigma F factor) [EC:2.7.11.1]
	Sporulation (Actinobacteria)	K06380	spoIIB; stage II sporulation protein B
	Sporulation (Actinobacteria)	K06381	spoIID; stage II sporulation protein D
	Sporulation (Actinobacteria)	K06382	spoIIE; stage II sporulation protein E [EC:3.1.3.16]
	Sporulation (Actinobacteria)	K06383	spoIIGA; stage II sporulation protein GA (sporulation sigma-E factor processing peptidase) [EC:3.4.23.-]
	Sporulation (Actinobacteria)	K06384	spoIIM; stage II sporulation protein M
	Sporulation (Actinobacteria)	K06385	spoIIP; stage II sporulation protein P
	Sporulation (Actinobacteria)	K06386	spoIIQ; stage II sporulation protein Q
	Sporulation (Actinobacteria)	K06387	spoIIR; stage II sporulation protein R
	Sporulation (Actinobacteria)	K06388	spoIISA; stage II sporulation protein SA
	Sporulation (Actinobacteria)	K06389	spoIISB; stage II sporulation protein SB
	Sporulation (Actinobacteria)	K06390	spoIIIAA; stage III sporulation protein AA
	Sporulation (Actinobacteria)	K06391	spoIIIAB; stage III sporulation protein AB
	Sporulation (Actinobacteria)	K06392	spoIIIAC; stage III sporulation protein AC
	Sporulation (Actinobacteria)	K06393	spoIIIAD; stage III sporulation protein AD
	Sporulation (Actinobacteria)	K06394	spoIIIAE; stage III sporulation protein AE
	Sporulation (Actinobacteria)	K06395	spoIIIAF; stage III sporulation protein AF

	Sporulation (Actinobacteria)	K06396	spoIIIAG; stage III sporulation protein AG
	Sporulation (Actinobacteria)	K06397	spoIIIAH; stage III sporulation protein AH
	Sporulation (Actinobacteria)	K06398	spoIVA; stage IV sporulation protein A
	Sporulation (Actinobacteria)	K06399	spoIVB; stage IV sporulation protein B [EC:3.4.21.116]
	Sporulation (Actinobacteria)	K06401	spoIVFA; stage IV sporulation protein FA
	Sporulation (Actinobacteria)	K06402	spoIVFB; stage IV sporulation protein FB [EC:3.4.24.-]
	Sporulation (Actinobacteria)	K06403	spoVAA; stage V sporulation protein AA
	Sporulation (Actinobacteria)	K06404	spoVAB; stage V sporulation protein AB
	Sporulation (Actinobacteria)	K06405	spoVAC; stage V sporulation protein AC
	Sporulation (Actinobacteria)	K06406	spoVAD; stage V sporulation protein AD
	Sporulation (Actinobacteria)	K06407	spoVAE; stage V sporulation protein AE
	Sporulation (Actinobacteria)	K06408	spoVAF; stage V sporulation protein AF
	Sporulation (Actinobacteria)	K06409	spoVB; stage V sporulation protein B
	Sporulation (Actinobacteria)	K06412	spoVG; stage V sporulation protein G
	Sporulation (Actinobacteria)	K06413	spoVK; stage V sporulation protein K
	Sporulation (Actinobacteria)	K06414	spoVM; stage V sporulation protein M
	Sporulation (Actinobacteria)	K06415	spoVR; stage V sporulation protein R
	Sporulation (Actinobacteria)	K06416	spoVS; stage V sporulation protein S

	Sporulation (Actinobacteria)	K06417	spoVID; stage VI sporulation protein D
	Sporulation (Actinobacteria)	K06437	yknT; sigma-E barrenled sporulation protein
	Sporulation (Actinobacteria)	K06438	yqfD; similar to stage IV sporulation protein
	Sporulation (Actinobacteria)	K07697	kinB; two-component system, sporulation sensor kinase B [EC:2.7.13.3]
	Sporulation (Actinobacteria)	K07698	kinC; two-component system, sporulation sensor kinase C [EC:2.7.13.3]
	Sporulation (Actinobacteria)	K07699	spo0A; two-component system, response regulator, stage 0 sporulation protein A
	Sporulation (Actinobacteria)	K08293	SMK1; sporulation-specific mitogen-activated protein kinase SMK1 [EC:2.7.11.24]
	Sporulation (Actinobacteria)	K08384	spoVD; stage V sporulation protein D (sporulation-specific penicillin-binding protein)
	Glycogen synthesis	K08822	GSK3A; glycogen synthase kinase 3 alpha [EC:2.7.11.26]
	Sporulation (Actinobacteria)	K12576	SPO12; sporulation-specific protein 12
	Sporulation (Actinobacteria)	K12771	SPS1; sporulation-specific protein 1 [EC:2.7.11.1]
	Sporulation (Actinobacteria)	K12772	SPS4; sporulation-specific protein 4
	Sporulation (Actinobacteria)	K12773	SPR3; sporulation-regulated protein 3
	Sporulation (Actinobacteria)	K12783	SSP1; sporulation-specific protein 1
	Sporulation (Actinobacteria)	K13532	kinD; two-component system, sporulation sensor kinase D [EC:2.7.13.3]
	Sporulation (Actinobacteria)	K13533	kinE; two-component system, sporulation sensor kinase E [EC:2.7.13.3]
	Glycogen synthesis	K16150	K16150; glycogen synthase [EC:2.4.1.11]
	Exopolysaccharide synthesis	K16566	exoY; exopolysaccharide production protein ExoY
	Exopolysaccharide synthesis	K16567	exoQ; exopolysaccharide production protein ExoQ
	Exopolysaccha	K16	exoZ; exopolysaccharide production protein ExoZ

	ride synthesis	568	
	Sporulation (Actinobacteria)	K16947	SPR28; sporulation-regulated protein 28
	Glycogen synthesis	K20812	glgA; glycogen synthase [EC:2.4.1.242]

537
538

539 Table A.4. Chlorophyll concentrations and water content values in the biocrust at each

540 sampling point and site.

Time	Chlorophyll concentration (mg chla/ g soil)	Water content (%)	Total organic carbon (%)	Total nitrogen (%)
T[0]	7.670	1.850	4.225	0.112
T[0]	8.553	2.670	4.107	0.114
T[0]	6.835	2.290	4.188	0.107
T[R]	10.145	13.610	2.999	0.104
T[R]	16.144	16.930	3.898	0.104
T[R]	15.703	16.550	3.787	0.109
T[R]	12.745	16.340	3.967	0.104
T[R]	14.160	17.520	3.972	0.071
T[1]	10.519	5.300	3.269	0.065
T[1]	16.003	5.620	3.238	0.065
T[1]	16.877	7.140	3.955	0.085
T[1]	15.262	6.220	3.964	0.073
T[1]	14.177	6.830	3.948	0.098
T[2]	10.092	3.920	3.879	0.087
T[2]	11.829	4.490	4.031	0.082
T[2]	11.840	4.510	4.244	0.100
T[2]	13.045	5.070	4.134	0.115
T[2]	12.975	6.900	4.050	0.095
T[3]	9.881	2.860	3.834	0.092
T[3]	12.751	3.670	3.709	0.100
T[3]	9.314	3.710	3.706	0.076
T[3]	9.366	4.320	4.511	0.081
T[3]	14.520	3.780	4.589	0.093

541
542

543 Table A.5. Dunn tests p values for chlorophyll concentration (mg chla/g of soil), water
544 content (%), total organic carbon content (%) and total nitrogen (%) in biocrust samples
545 collected at the different sampling point. Bold numbers mark significant differences (<0.05).

Comparison	Chlorophyll	Water content	Total organic Carbon	Total Nitrogen
T[0] - T[1]	**0.00538004**	0.05699315	0.89	0.169
T[0] - T[2]	**0.02846706**	0.35971877	0.64	0.525
T[1] - T[2]	0.25895220	**0.02620581**	0.55	0.448
T[0] - T[3]	0.17516547	0.20434975	0.75	0.065
T[1] - T[3]	0.05299877	**0.00804845**	0.85	0.611
T[2] - T[3]	0.16605599	0.32025932	0.43	0.210
T[0] - T[R]	**3.5589E-06**	0.15725837	0.84	0.723
T[1] - T[R]	**0.02620581**	0.28273460	0.95	0.300
T[2] - T[R]	**0.00485039**	0.08612648	0.51	0.776
T[3] - T[R]	**0.00018814**	**0.03347764**	0.90	0.128

546

547 Table A.6. Relative abundance of the taxa in the biocrust community at each time point.

Phylum	Order	Time Point	Relative Abundance
Actinobacteria	Frankiales	T[0]	0.022907633
		T[R]	0.03574372
		T[1]	0.012995761
		T[2]	0.032045929
		T[3]	0.02063487
	IMCC26256	T[0]	0.009681202
		T[R]	0.005259368
		T[1]	0.008388448
		T[2]	0.008617354
		T[3]	0.006227356
	Micrococcales	T[0]	0.385359194
		T[R]	0.009765818
		T[2]	0.008171044
		T[3]	0.00669884
	Micromonosporales	T[R]	0.013939918
		T[1]	0.005556665
		T[2]	0.007483088
		T[3]	0.007512356
	Microtrichales	T[1]	0.00532056
		T[2]	0.005352285
	Propionibacteriales	T[R]	0.010647015
		T[1]	0.006196615
		T[2]	0.009500737
		T[3]	0.005302327
	Pseudonocardiales	T[R]	0.007935732
		T[2]	0.005403369
	Rubrobacterales	T[0]	0.015244484
		T[R]	0.075369688
		T[1]	0.088221276
		T[2]	0.103851434
		T[3]	0.08049968
	Solirubrobacterales	T[0]	0.076522403
		T[R]	0.039879122
		T[1]	0.043060268
		T[2]	0.045998142
		T[3]	0.031839496
Cyanobacteria	Chloroplast	T[0]	0.020862309
		T[R]	0.011650182
		T[1]	0.026512447
		T[2]	0.028141321
		T[3]	0.018079461
	Cyanobacteriales	T[0]	0.19073226
Cyanobacteria	Cyanobacteriales	T[R]	0.389427243

		T[1]	0.333676493
		T[2]	0.292463654
		T[3]	0.350595706
	Unknown Oxyphotobacteria	T[R]	0.013481119
		T[1]	0.015453064
		T[2]	0.013590863
		T[3]	0.015066421
	Thermosynechococcales	T[0]	0.010799313
Acidobacteriota	Bryobacterales	T[R]	0.005153526
Bacteroidota	Chitinophagales	T[0]	0.006236605
		T[R]	0.005163481
		T[2]	0.007262191
	Cytophagales	T[0]	0.009163053
		T[R]	0.096453172
		T[1]	0.11996715
		T[2]	0.079192234
		T[3]	0.090668802
Chloroflexi	Kallotenuales	T[R]	0.00838268
		T[2]	0.01633687
		T[3]	0.008408777
	Thermomicrobiales	T[2]	0.005146914
Gemmatimonadota	Gemmatimonadales	T[R]	0.005436359
		T[2]	0.006908222
	Longimicrobiales	T[R]	0.016006999
		T[2]	0.005421611
Myxococcota	Haliangiales	T[R]	0.005678943
		T[3]	0.006010924
	Myxococcales	T[R]	0.020299082
		T[1]	0.010755355
		T[2]	0.013671351
		T[3]	0.014621574
	Nannocystales	T[R]	0.008809035
		T[1]	0.01090915
		T[2]	0.005558526
		T[3]	0.006743362
	Polyangiales	T[R]	0.008294912
		T[1]	0.008084686
		T[2]	0.005990088
		T[3]	0.006645987
Proteobacteria	Acetobacterales	T[R]	0.014783181
		T[1]	0.012028303
		T[2]	0.016252769
		T[3]	0.016407297
	Azospirillales	T[0]	0.030702093
	Burkholderiales	T[0]	0.056796051
Proteobacteria	Burkholderiales	T[R]	0.012959379

		T[1]	0.010671657
		T[2]	0.013591631
		T[3]	0.012713217
	Caulobacterales	T[0]	0.012899179
		T[R]	0.022042144
		T[1]	0.034822507
		T[2]	0.020704156
		T[3]	0.024863575
	Pseudomonadales	T[0]	0.013867311
	Rhizobiales	T[0]	0.087344626
		T[R]	0.043724525
		T[1]	0.063099159
		T[2]	0.070129812
		T[3]	0.068004988
	Rhodobacterales	T[0]	0.00551081
		T[R]	0.016305263
		T[1]	0.016673137
		T[2]	0.021005185
		T[3]	0.016425317
	Sphingomonadales	T[0]	0.018796014
		T[R]	0.038019558
		T[1]	0.044013044
		T[2]	0.044435076
		T[3]	0.033523863
Verrucomicrobiota	Chthoniobacterales	T[R]	0.012024879
		T[1]	0.066714297
		T[2]	0.044130375
		T[3]	0.094877543

548
549
550
551

552 Table A.7. P-values of the Dunn tests between time points on the relative abundance of the

553 actinobacterial and cyanobacterial orders. Bold numbers are significant (<0.05).

Comparison	Cyanobacteria	Actinobacteria
T[0] - T[1]	**6.13E-10**	**8.15E-13**
T[0] - T[2]	**5.13E-08**	**2.52E-14**
T[0] - T[3]	**5.98E-10**	**6.89E-11**
T[0] - T[R]	**6.52E-10**	**6.47E-14**
T[1] - T[3]	0.498128567	0.228324880
T[1] - T[2]	0.191797281	0.294405229
T[1] - T[R]	0.495469243	0.345672443
T[2] - T[R]	0.194912395	0.442935801
T[3] - T[R]	0.493597980	0.126850627
T[2] - T[3]	0.190519550	0.099407424

554
555

556 Table A.8. Abundance (in copy number (CN)) of each time points within each group of gene.

Gene Group	Time points	Abundance
DNA conservation	T[0]	20590
	T[R]	91433
	T[1]	92496
	T[2]	78321
	T[3]	81983
DNA repair and degradation	T[0]	13579
	T[R]	66132
	T[1]	67048
	T[2]	55948
	T[3]	58457
Light energy or sensing	T[0]	85
	T[R]	43
	T[1]	59
	T[2]	64
	T[3]	17
Lithotrophs	T[0]	7554
	T[R]	37972
	T[1]	38632
	T[2]	31341
	T[3]	32758
Nitrogen	T[0]	10027
	T[R]	50708
	T[1]	58068
	T[2]	48225
	T[3]	45638
Organotrophs	T[0]	60007
	T[R]	108275
	T[1]	111044
	T[2]	88557
	T[3]	89148
Phototrophy	T[0]	50301
	T[R]	445432
	T[1]	425819
	T[2]	342188
	T[3]	407532
ROS-damage prevention	T[0]	26126
	T[R]	138367
	T[1]	143726
	T[2]	121507
	T[3]	126677
Sensing & motility	T[0]	31075
	T[R]	81947
	T[1]	92070

Sensing & motility	T[2]	90844
	T[3]	74436
Sporulation capsule & C-storage	T[0]	7302
	T[R]	48141
	T[1]	48944
	T[2]	38998
	T[3]	42341

557

558 Table A.9. Chi-square values and p-values of the Dunn tests between time points done on the

559 functional prediction results. Bold numbers are significant (< 0.05)

Comparison	DNA Conservation	DNA Repair	Light energy	Lithotrophy	Nitrogen
T[0] - T[1]	**0.00489293**	**0.00293591**	0.19388801	**0.00030834**	**4.22E-17**
T[0] - T[2]	**0.02033475**	**0.0097339**	0.44831059	**0.00749298**	**8.12E-12**
T[0] - T[3]	**0.02906312**	**0.01558465**	0.2755365	**0.01520981**	**8.15E-10**
T[0] - T[R]	**0.02863121**	**0.00520412**	0.37990911	**0.00162909**	**1.30E-12**
T[1] - T[3]	0.21328302	0.24422913	**0.04593218**	0.072911	**0.00403999**
T[1] - T[2]	0.26782432	0.31450078	0.19843215	0.12613918	**0.03331074**
T[1] - T[R]	0.21549186	0.41187192	0.25970621	0.28894927	0.06264837
T[2] - T[3]	0.43027457	0.41697806	0.20090041	0.37842665	0.20768207
T[2] - T[R]	0.43325114	0.3972775	0.41957403	0.27813996	0.38159137
T[3] - T[R]	0.49697916	0.31916653	0.14884666	0.184595	0.13225512
Chi-square	7.021623874	8.913054423	2.944440598	12.94456096	75.97487673

Comparisons	Organotrophy	Phototrophy	ROS	Motility	Sporulation
T[0] - T[1]	**0.00189691**	**5.38E-36**	**5.70E-06**	**1.09E-18**	**7.48E-05**
T[0] - T[2]	**0.02110913**	**8.46E-17**	**2.77E-05**	**2.10E-14**	**3.01E-09**
T[0] - T[3]	**0.04112206**	**8.77E-26**	**8.96E-05**	**2.41E-11**	**0.0008838**
T[0] - T[R]	**0.01948721**	**4.27E-35**	**6.29E-05**	**1.22E-14**	**0.00040669**
T[1] - T[3]	0.09077588	**0.00930641**	0.22920864	**0.00608522**	0.22132375
T[1] - T[2]	0.15937532	**5.23E-07**	0.33993514	0.08422197	**0.00969216**
T[1] - T[R]	0.16882618	0.42394382	0.26107583	0.09739203	0.30432515
T[2] - T[3]	0.3673185	**0.00570786**	0.37114762	0.12925022	**0.00094887**
T[2] - T[R]	0.48475837	**1.36E-06**	0.41005945	0.46785414	**0.00218557**
T[3] - T[R]	0.35302059	**0.01533294**	0.45960721	0.11302291	0.39907998
Chi-square	8.60329063	195.4178784	22.91571278	87.21260295	34.5684137

560
561

562

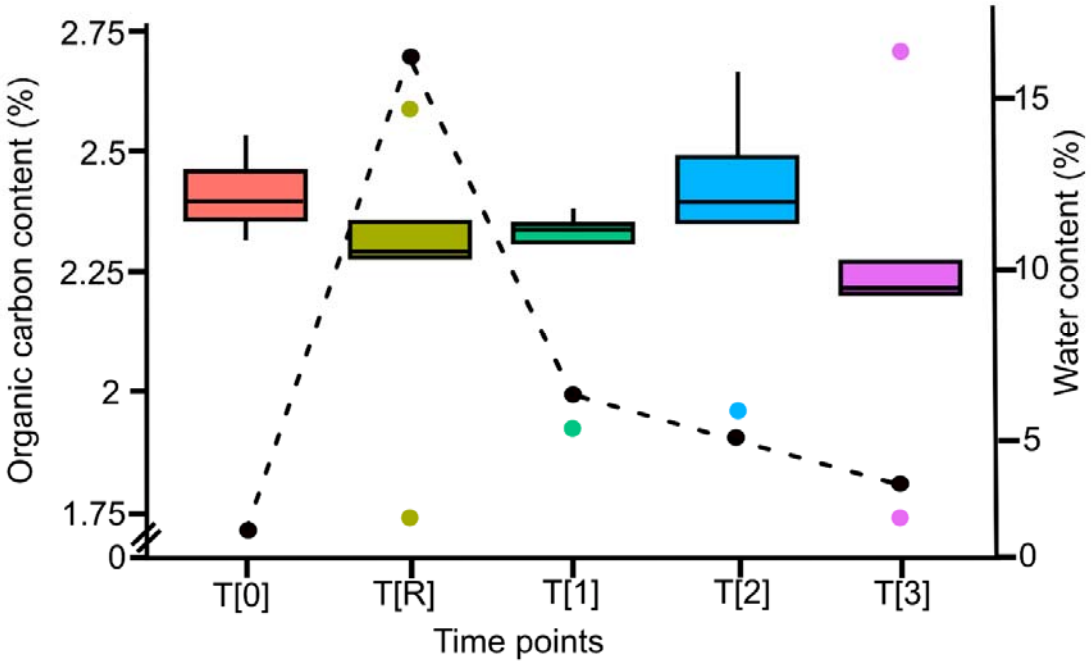

563
564 Figure A.1. Barplot of the organic carbon content for each sampling point.
565
566

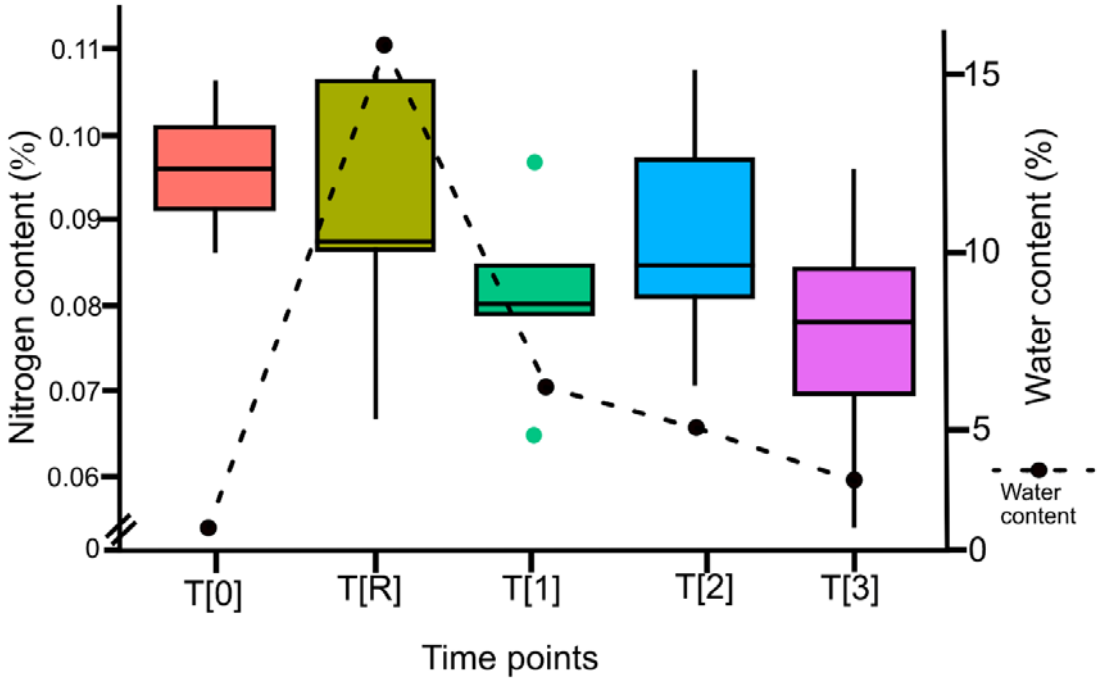

Figure A.2. Barplot of the nitrogen content (in g) for each time point.


Tyre
LEBANON
SYRIA
Haifa
North District
Daraa Governorate
As Suwayda
Haifa District
Irbid
Netanya
Nablus
Ajlun
Jarash
Tel Aviv
Holon
Rishon LeZion
Zarqa
Ramallah
Balqa
Amman
Ashdod
Jerusalem
Ashkelon
Gaza
Hebron
Madaba
Amman
Area H2
Khan Yunis
Beersheba
Al 'Arish
South District
North Sinai
Maan
EGYPT

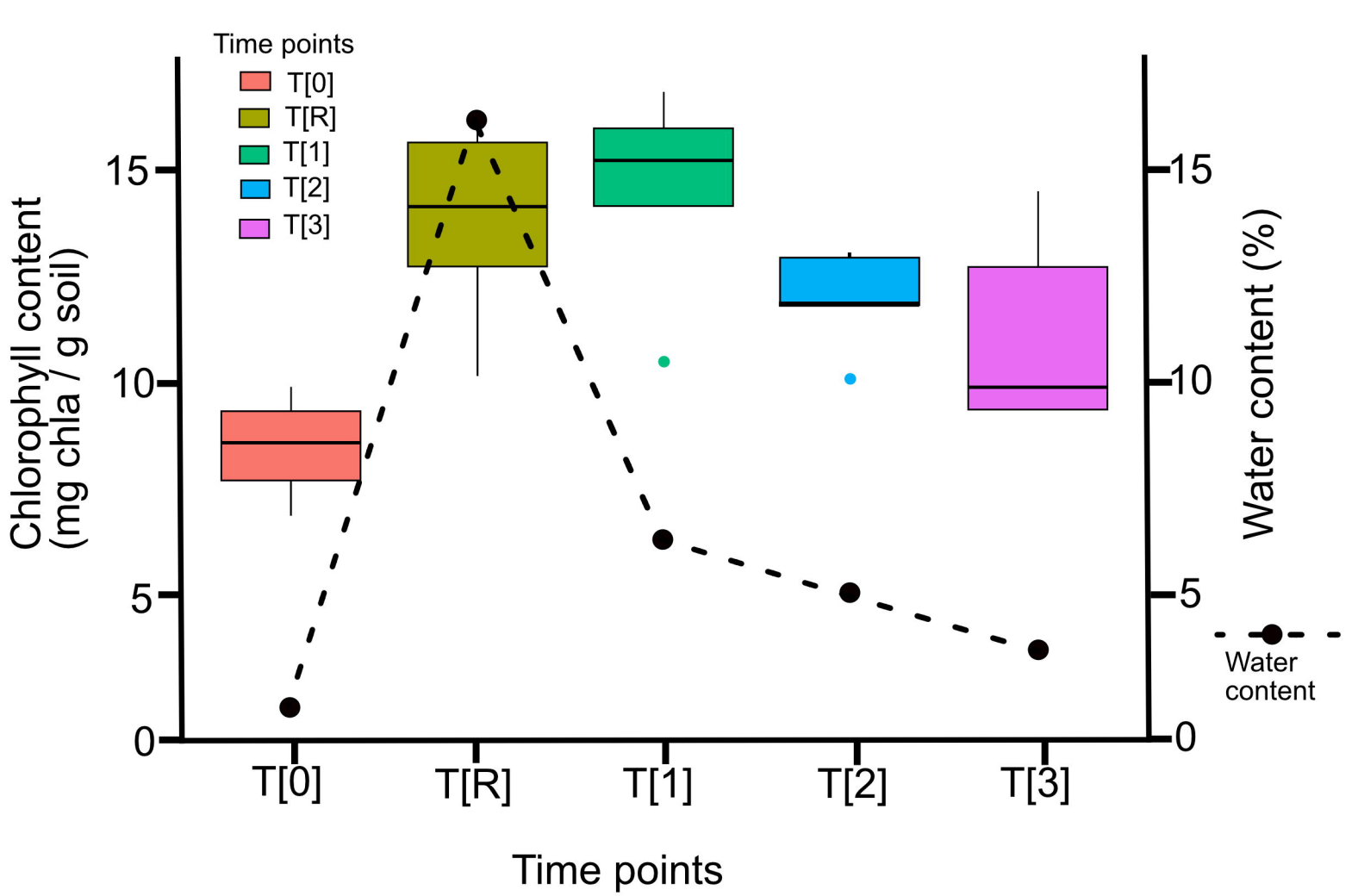
Time points
T[0]
T[R]
T[1]
T[2]
T[3]
Chlorophyll content
(mg chla / g soil)
Water content (%)
Water
content
0
5
10
15
T[0]
T[R]
T[1]
T[2]
T[3]
Time points

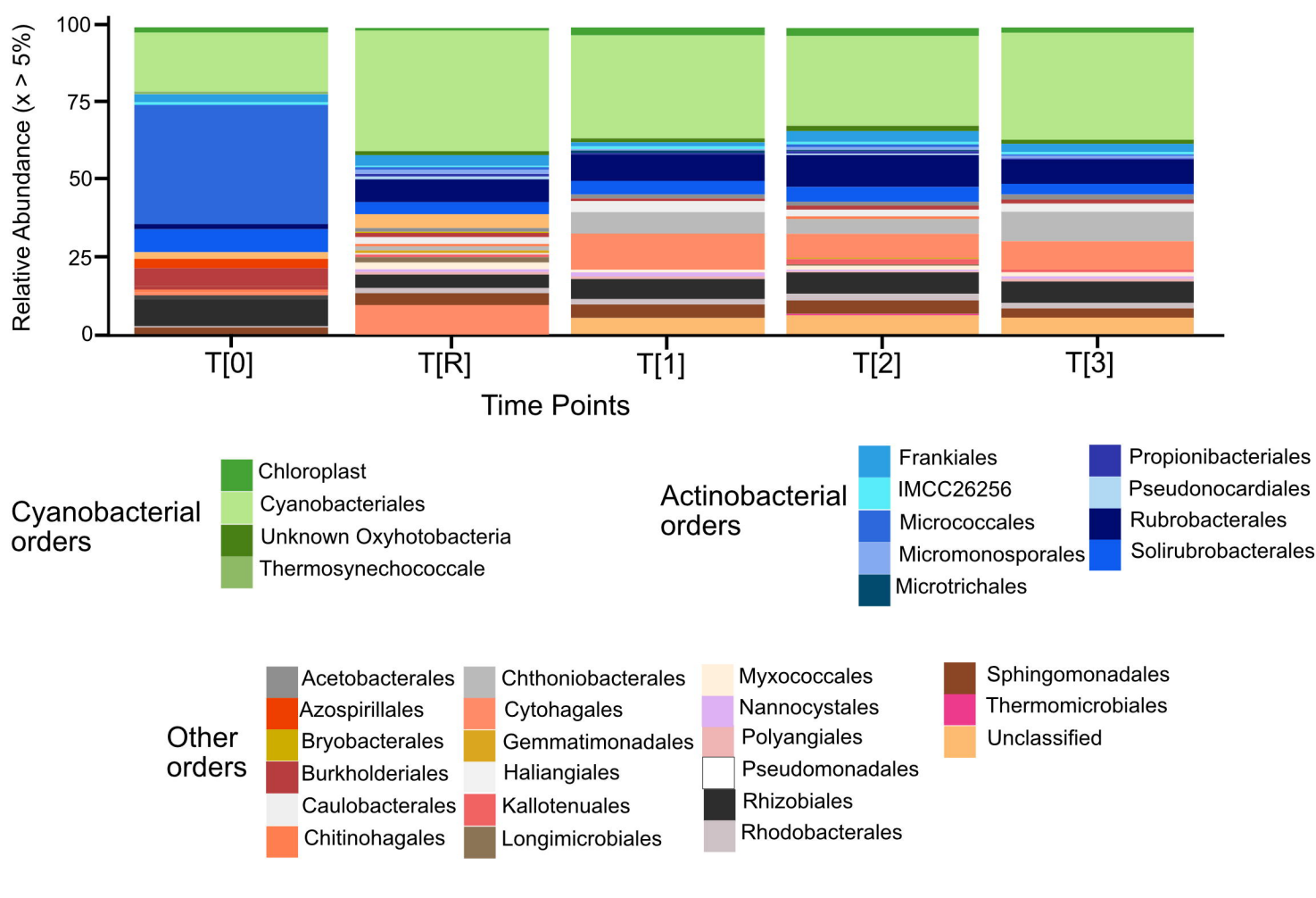
Relative Abundance (x > 5%)
100
75
50
25
0
T[0]
T[R]
T[1]
T[2]
T[3]
Time Points
Cyanobacterial orders
Chloroplast
Cyanobacteriales
Unknown Oxyhotobacteria
Thermosynechococcale
Actinobacterial orders
Frankiales
IMCC26256
Micrococcales
Micromonosporales
Microtrichales
Propionibacteriales
Pseudonocardiales
Rubrobacterales
Solirubrobacterales
Other orders
Acetobacterales
Azospirillales
Bryobacterales
Burkholderiales
Caulobacterales
Chitinohagales
Chthoniobacterales
Cytohagales
Gemmatimonadales
Haliangiales
Kallotenuales
Longimicrobiales
Myxococcales
Nannocystales
Polyangiales
Pseudomonadales
Rhizobiales
Rhodobacterales
Sphingomonadales
Thermomicrobiales
Unclassified

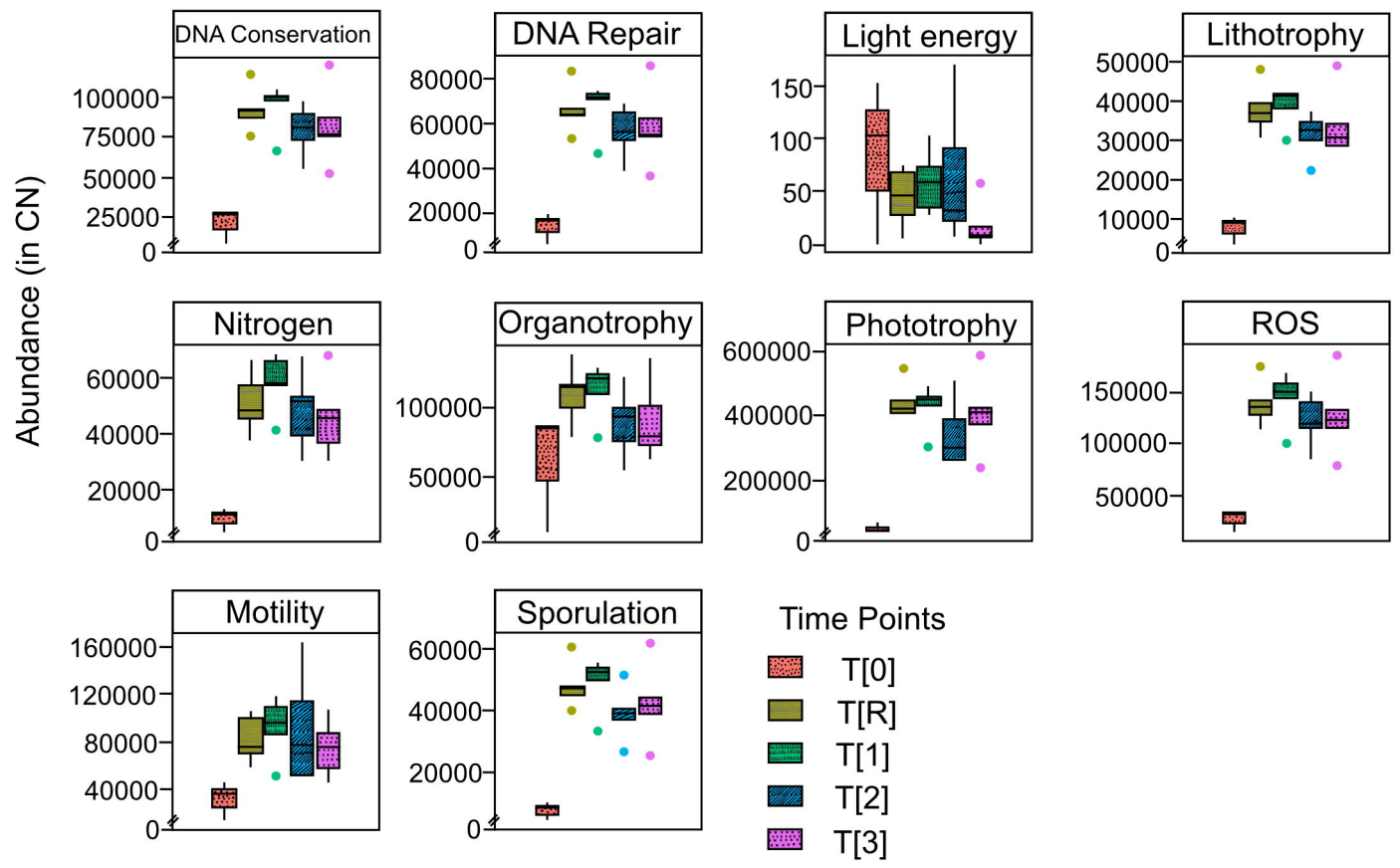
Abundance (in CN)
DNA Conservation
DNA Repair
Light energy
Lithotrophy
Nitrogen
Organotrophy
Phototrophy
ROS
Motility
Sporulation
Time Points
T[0]
T[R]
T[1]
T[2]
T[3]